# Triclosan depletes the membrane potential in *Pseudomonas aeruginosa* biofilms inhibiting aminoglycoside induced adaptive resistance

Michael M. Maiden and Christopher M. Waters*

[1]Departments of Microbiology and Molecular Genetics and The BEACON Center for The Study of Evolution in Action, Michigan State University, East Lansing, Michigan, United States of America

*Corresponding Author

E-mail: watersc3@msu.edu (CW)

**Abstract**

Biofilm-based infections are difficult to treat due to their inherent resistance to antibiotic treatment. Discovering new approaches to enhance antibiotic efficacy in biofilms would be highly significant in treating many chronic infections. Exposure to aminoglycosides induces adaptive resistance in *Pseudomonas aeruginosa* biofilms. Adaptive resistance is primarily the result of active antibiotic export by RND-type efflux pumps, which use the proton motive force as an energy source. We show that the protonophore uncoupler triclosan depletes the membrane potential of biofilm growing *P. aeruginosa,* leading to decreased activity of RND-type efflux pumps. This disruption results in increased intracellular accumulation of tobramycin and enhanced antimicrobial activity *in vitro*. In addition, we show that triclosan enhances tobramycin effectiveness *in vivo* using a mouse wound model. Combining triclosan with tobramycin is a new anti-biofilm strategy that targets bacterial energetics, increasing the susceptibility of *P. aeruginosa* biofilms to aminoglycosides.

**Author summary**

Adaptive resistance is a phenotypic response that allows *P. aeruginosa* to transiently survive aminoglycosides such as tobramycin. To date, few compounds have been identified that target adaptive resistance. Here, we show the protonophore uncoupler triclosan disrupts the membrane potential of *P. aeruginosa*. The depletion of the membrane potential reduces efflux pump activity, which is essential for adaptive resistance, leading to increased tobramycin accumulation and a shorter onset of action. Our results demonstrate that in addition to its canonical mechanism inhibiting membrane biosynthesis, triclosan can exert antibacterial properties by functioning as a protonophore that targets *P. aeruginosa* energetics.

## Introduction

*Pseudomonas aeruginosa* is a Gram-negative opportunistic pathogen that can form highly recalcitrant biofilms in immunocompromised hosts such as those suffering from cystic fibrosis (CF) and diabetes (1-4). Biofilms are a community of cells enmeshed in a self-made matrix that is highly tolerant to antibiotic treatment (1-4). In addition to biofilm growth, *P. aeruginosa* possesses many antibiotic resistance mechanisms including low outer membrane (OM) permeability, which is estimated to be 1/100$^{th}$ that of *Escherichia coli* (5), the expression of proton motive force (PMF) dependent resistance-nodulation-cell division (RND) family of multidrug efflux pumps, and a chromosomal encoded AmpC β-lactamase, making it naturally resistant to β-lactams (4).

*P. aeruginosa* also exhibits a unique form of adaptive resistance in response to aminoglycosides, cationic antimicrobial peptides, and polymyxins (6, 7). Adaptive resistance is mainly mediated by the induction of RND-type efflux pumps and by alterations to the OM within 2-hrs of exposure to subinhibitory concentrations of aminoglycosides (8-11). Aminoglycosides cause the mistranslation of the PA5471 leader peptide PA5471.1, a peptide which inhibits the MexZ repressor, thereby triggering the induction of the RND-type efflux pump MexXY (12). This phenomenon has been observed *in vitro*, in animal models, and in CF patients (13-17).

Aminoglycoside uptake occurs in three steps (18-20). In the first step, termed "self-promoted uptake," positively charged aminoglycosides bind negatively charged components of the OM, triggering permeabilization and diffusion (18-20). In the second step, energy dependent phase-I (EDP-I), aminoglycosides slowly cross the inner membrane (IM) dependent upon the membrane potential ($\Delta\psi$) (18-20). In the third step, EDP-II, aminoglycosides bind to the A-site

of the 30S subunit of membrane-associated ribosomes and cause the synthesis of misfolded proteins that insert into the IM triggering permeabilization of the cytosolic barrier (18-20). This leads to an irreversible entry of aminoglycosides into the cell, thereby inhibiting translation.

Despite the well-documented phenomenon of adaptive resistance, aminoglycosides continue to be the standard of care for pseudomonal infections (21). In fact, pulmonary infections in CF patients are treated with extended doses of the aminoglycoside tobramycin (300-mg nebulized twice-a-day for 28-days), reaching mean sputum concentrations of ~737 µg/g per dose (21, 22). As antibacterial resistance continues to be an emerging public health crisis, there is a crucial need for new therapeutic approaches that decrease resistance (23). One approach is to target bacterial energetics (24). The feasibility of this approach was recently demonstrated by the discovery of the protonophore uncoupler bedaquiline, which is the first new Food and Drug Administration (FDA) approved *Mycobacterium tuberculosis* (*Mtb*) drug in 40-years (25-27).

We previously performed a high throughput screen (HTS) to identify compounds that enhanced tobramycin against *P. aeruginosa* biofilms and unexpectedly discovered that the combination of triclosan and tobramycin (or other aminoglycosides) was 100-times more effective than either triclosan, tobramycin, or other aminoglycosides alone at killing established *P. aeruginosa* biofilms (28). Triclosan is a fatty acid synthesis inhibitor, targeting the enoyl-acyl carrier reductase FabI (29). However, it is well-known that *P. aeruginosa* is inherently resistant to triclosan due to the expression of both the RND-type efflux pump TriABC and a triclosan resistant enoyl-acyl carrier reductase FabV, and our previous results suggested that triclosan does not enhance tobramycin activity by targeting FabI (28, 30, 31). Therefore, the mechanism of action of triclosan enhancement of aminoglycoside activity remained unknown.

The PMF is the sum of the membrane potential due to charge separation ($\Delta\psi$, positive$_{outside}$/negative$_{inside}$) and the proton gradient ($\Delta$pH, acidic$_{outside}$/alkaline$_{inside}$) across the inner membrane (32, 33). Recently, it has been shown that in addition to fatty acid synthesis inhibition, triclosan possesses protonophore activity that can disrupt the $\Delta\psi$ of mitochondria isolated from rats, artificial bilayer lipid membranes, and the Gram-positive bacterium *Bacillus subtilis* (34-38). This led us to hypothesize that triclosan enhances aminoglycoside activity by targeting the $\Delta\psi$ in *P. aeruginosa* (28). In fact, from the same HTS in which triclosan was identified, we discovered that the protonophore uncoupler oxyclozanide acted synergistically with tobramycin to kill *P. aeruginosa* biofilms (39).

Here we demonstrate that triclosan increases *P. aeruginosa* susceptibility to tobramycin by disrupting adaptive resistance. This occurs because triclosan decreases the $\Delta\psi$, leading to a reduction in the activity of RND-type efflux pumps, which increases tobramycin accumulation within cells. Finally, we demonstrate that triclosan in combination with tobramycin embedded in a hydrogel is effective *in vivo* using a murine wound model. As numerous toxicity studies have demonstrated that triclosan is safe when used appropriately (40-42), this combination has the clinical potential to improve the treatment of biofilm-based infections by targeting bacterial energetics.

## Results

### The disruption of fatty acid synthesis does not increase *P. aeruginosa* susceptibility to tobramycin.

To determine if the inhibition of fatty acid biosynthesis and membrane biogenesis by triclosan is responsible for increasing *P. aeruginosa* susceptibility to tobramycin, we tested if the specific fatty acid synthesis inhibitor AFN-1252 synergized with tobramycin to kill *P. aeruginosa* biofilms. AFN-1252 forms a binary complex with the active site of FabI, which is an enoyl-acyl reductase responsible for the final elongation step in fatty acid synthesis and is inhibited by triclosan (43).

AFN-1252 alone and in combination with tobramycin was not effective at killing biofilms (Fig. S1). At the maximal concentrations of tobramycin and AFN-1252 used we observed slightly more than 2-fold killing; however, this difference was not statistically significant and far weaker than the ~100-fold killing observed when triclosan is combined with tobramycin (28). These findings are in agreement with our previous genetic experiments using a FabI mutant of *P. aeruginosa* that showed identical resistance to tobramycin treatment as the parental strain (28). Together, both our genetic and molecular experiments suggest that the inhibition of FabI by triclosan does not account for increased *P. aeruginosa* susceptibility to tobramycin.

### Triclosan combined with tobramycin causes synergistic permeabilization of cells within biofilms.

Aminoglycosides corrupt protein synthesis by binding to the A-site of the 30S subunit of membrane bound ribosomes causing mistranslation of membrane proteins and inner membrane

permeabilization (18-20). We initially hypothesized that triclosan enhanced tobramycin killing by permeabilizing cells in biofilms. To test this hypothesis, we stained cells with the cell-impermeant TO-PRO™-3 iodide dye, which selectively emits a fluorescent signal in permeabilized cells.

Treatment for 2-hrs with triclosan or tobramycin alone resulted in ~15% and ~11% of the cells within biofilms to become permeabilized, respectively (Fig. 1). Neither of these increases were statistically significantly compared to untreated controls. Alternatively, the combination of triclosan and tobramycin permeabilized ~50% of cells after only 2-hrs of treatment. This result suggests that neither triclosan nor tobramycin treatment alone is sufficient to permeabilize *P. aeruginosa* cells growing in biofilms.

**Mutations in *fusA1* are resistant to the combination.**

To further elucidate the mechanism of action of this combination, we selected for resistance mutants and then performed whole genome sequencing to identify causative mutations, using a modified method developed by Lindsey et al. (44). 27 *P. aeruginosa* biofilms serially passaged in parallel were exposed to sudden, moderate and gradual treatment regimens consisting of ever-increasing concentrations of tobramycin and triclosan (Table S1). No resistant mutations were isolated from populations exposed to sudden or moderate treatment regimens. After 30 passages, two resistant populations from the gradual treatment regimen were isolated (Table 1), and 96-colonies were isolated from each mutant pool that were found to be resistant to the combination.

To determine the mutation(s) responsible for the resistance to the combination we performed whole genome sequencing on two mutants from the F1 and four mutants from the B2

mutant populations (Table 1). These 6 mutants all showed complete resistance to tobramycin and partial resistance to the combination compared to the ancestral strain (Fig. 2). The low level of killing generated by the combination may be attributed to triclosan as all six of these mutants exhibited increased sensitivity to triclosan treatment alone versus the ancestral strain. This phenomenon, termed "collateral sensitivity," is the process by which resistance to one antimicrobial simultaneously results in increased sensitivity to unrelated antimicrobials (45).

One common feature of all six mutants was a single nucleotide polymorphism (SNP) in the *fusA1* gene encoding for EF-G1A, a protein responsible for ribosomal translocation and recycling (46). Two unique mutations, a SNP at residues L40Q or T64A were identified. These mutations are near or within the switch I domain, respectively, which is required for hydrolysis of guanosine triphosphate and the "power-stroke" of EF-G1A. Because all mutants having a L40Q SNP came from mutant pool F1 and all mutants having a T64A SNP came from mutant pool B2, we hypothesize that these SNPs occurred early on during selection, allowing for clonal expansion. However, no two isolates have the exact same set of SNPs, indicating the sequenced strains are not siblings and each isolate is a distinct mutant as detailed in the discussion (supplemental spreadsheet). Importantly, mutations in *fusA1* that have been found in clinical isolates, including L40Q, confer resistance to tobramycin through an unknown mechanism (47). Together, these results suggest that tobramycin is the component of the combination that is primarily responsible for killing.

**Initial tobramycin treatment is required for the combination to be effective.**

The corruption of translation is thought to be the first step in aminoglycoside induced adaptive resistance (12). This led us to hypothesize that tobramycin must first corrupt translation

thereby triggering adaptive resistance and the induction of RND-type efflux pumps for the combination to be synergistic (8-10, 12). To test if tobramycin induction of adaptive resistance was important for synergy, we first treated *P. aeruginosa* biofilms with tobramycin alone for 3-hrs and then washed the biofilms three time in Dulbecco's Phosphate Buffer Solution (DPBS) for 3-mins each followed by subsequent treatment with triclosan alone for 3-hrs. We performed a similar experiment first treating with triclosan followed by tobramycin treatment.

Sequential treatment with tobramycin followed by triclosan addition caused synergy, resulting in ~2-$\log_{10}$ reduction in cells within biofilms compared to untreated controls (Fig. S2). Intriguingly, despite no longer having tobramycin in the media, the cells within the biofilms were killed when treated with triclosan. We speculate that enough tobramycin remains after washing due to association of aminoglycosides with the extracellular polymeric substances (EPSs) making up the biofilm matrix and cell itself, which has been demonstrated to be resistant to removal by washing (19, 48). Alternatively, initial treatment with triclosan followed by treatment with tobramycin did not cause synergy or result in significant biofilm killing. These data suggest that a phenotypic switch induced by aminoglycoside exposure is important for synergistic activity.

In support of these experiments, we previously showed that tobramycin induces classic adaptive resistance, rendering *P. aeruginosa* refractory to killing by tobramycin until 6-hours, with the greatest resistance observed at 2-hrs (28). Furthermore, we found that only antibiotics that corrupt translation (aminoglycosides and tetracycline) act synergistically or are enhanced when combined with triclosan (28). Our past and current results lead us to hypothesize that tobramycin triggers adaptive resistance, which is then disrupted by triclosan.

**Triclosan reduces RND-type efflux pump activity.**

Because RND-type efflux pumps are a major component of aminoglycoside induced adaptive resistance (8-10, 12), we measured their activity in biofilms after treatment with tobramycin alone or in combination with triclosan by measuring cellular accumulation of ethidium bromide. Ethidium bromide is a substrate of RND-type efflux pumps, and its accumulation within cells can be used as a proxy for their activity (49). In this assay, the protonophore carbonyl cyanide 3-chlorophenylhydrazone (CCCP), which is known to reduce efflux pump activity, was used as a positive control (49). CCCP treatment led to increased ethidium bromide accumulation in *P. aeruginosa* biofilms as expected (Fig. 3). Similarly, triclosan reduced efflux pump activity as indicated by increased ethidium bromide accumulation, but tobramycin treatment alone had no effect. The combination of triclosan and tobramycin was similar to triclosan alone. These data suggest that triclosan reduces the activity of RND-type efflux pumps.

**Triclosan increased intercellular accumulation of tobramycin.**

Triclosan inhibition of RND-type efflux pumps should increase the accumulation of tobramycin within cells. To test this, we conjugated tobramycin with the fluorescent Texas Red dye (TbTR) as previously described (50), and measured its accumulation within cells growing as biofilms. Conversely, we also measured TbTR extrusion from cells into treatment-free recovery media.

For accumulation assays, biofilms were treated with TbTR with and without triclosan for 30-mins. Based on our previously published time-killing studies, this time point is before the

combination causes cell death (28). Prior to reading fluorescence, biofilms were washed, mechanically disrupted with a wooden stick, and cells were lysed to release TbTR. Triclosan in combination with TbTR resulted in a statistically significant increase in TbTR accumulation whereas CCCP did not significantly increase TbTR accumulation (Fig. 4A). This is in agreement with CCCPs reduced potency compared to triclosan at disrupting the membrane potentials of bacteria due to differences in lipophilicity and reduced activity against RND-type efflux pumps in *P. aeruginosa* biofilms (36).

To confirm that co-treatment with triclosan increased tobramycin accumulation within cells, biofilms were treated with TbTR with and without triclosan for 30-mins. Then biofilms were washed three-times in DPBS, recovered in treatment-free media for 30-mins and the supernatant was measured. Triclosan in combination with TbTR resulted in greater overall extrusion into treatment-free media, indicating more TbTR had accumulated in cells prior to recovery (Fig. 4B). These results support the conclusion that triclosan reduces the activity of RND-type efflux pumps, leading to increased accumulation of TbTR within cells.

**Triclosan inhibits tobramycin induced Δψ.**

Triclosan has a hydroxyl group with a dissociable proton that can disrupt the Δψ in eukaryotic cells, mitochondria, and bacteria (34-38). Because adaptive resistance is primarily the result of PMF driven RND-type efflux pumps (8-10, 12), we speculated that the depletion of the Δψ could lead to their inhibition and the abolishment of adaptive resistance. In these experiments, we measured changes in the Δψ rather than the ΔpH because at neutral pH the PMF in bacteria is primarily composed of the Δψ due to homeostatic buffering (51, 52), and RND-type efflux pump activity is primarily driven by the Δψ which is generated more rapidly than

ΔpH (53, 54). To measure changes in the Δψ of *P. aeruginosa* growing as biofilms, cells were stained with the fluorescent Δψ indicator DiOC2(3) dye and analyzed by flow cytometry. Cells were also co-stained with the membrane impermeant TO-PRO™-3 iodide dye to exclude permeabilized cells from analysis of Δψ.

Triclosan treatment for 2-hrs reduced the population of cells maintaining a Δψ 4-fold, from ~20% to ~5% (Fig. 5). Tobramycin treatment resulted in an increase in the population of cells with a Δψ almost 2-fold, from ~20% to ~37%. This increase is indicative of adaptive resistance (8-10, 12). Triclosan in addition to tobramycin reduced the population of cells maintaining a Δψ almost 4-fold from tobramycin treatment alone to levels comparable to untreated biofilms. These data suggest that triclosan depletes the Δψ at an essential time in aminoglycoside induced adaptive resistance when a surge in the Δψ is protective against tobramycin by increasing RND-type efflux pump activity.

**Methyl-triclosan does not disrupt the membrane potential or synergize with tobramycin.**

To confirm that protonophore activity by triclosan is responsible for tobramycin enhancement, we treated cells with the chemical derivative methyl-triclosan, which lacks the hydroxyl moiety necessary for gaining and losing a proton and therefore cannot act as a protonophore (35). In addition, without this hydroxyl group, methyl-triclosan cannot inhibit fatty acid synthesis by forming a complex with the co-factors NADH/NAD+ (35).

We first performed biofilm susceptibility testing using methyl-triclosan alone and in combination with tobramycin. Neither methyl-triclosan nor the combination were effective against biofilms after 6-hrs of treatment over a range of concentrations (Fig. S3). Furthermore, methyl-triclosan had no effect on the population of cells maintaining a Δψ compared to untreated

biofilms and did not reduce the tobramycin induced surge in Δψ after 2-hrs of treatment (Fig. S4A). In addition, methyl-triclosan did not cause permeabilization of cells alone or in combination with tobramycin (Fig. S4B). Likewise, methyl-triclosan was unable to significantly reduce efflux pump activity (Fig. S5). These results support the conclusion that triclosan protonophore activity is required for the depletion of the tobramycin induced Δψ surge and inhibition of RND-type efflux pump activity.

**ATP Depletion does not render cells more sensitive to tobramycin.**

Another outcome of triclosan depleting the Δψ would be decreased energy generation, which could contribute to the sensitivity of biofilms to tobramycin. We performed antimicrobial susceptibility assays on 24-hr old biofilms grown in rich medium that were then DPBS-starved for 5 days. We observed the same synergy of the combination in these conditions as treatment with triclosan or tobramycin alone failed to cause bacterial killing whereas the combination of triclosan and tobramycin caused significant killing (Fig. S6). These data suggest that the disruption of the Δψ by triclosan does not induce synergy by depletion of ATP.

**Triclosan and tobramycin show enhanced efficacy in an *in vivo* wound model.**

To determine if triclosan and tobramycin are more effective against biofilms *in vivo,* we tested their activity using a murine wound model (55, 56). In this model, a 1-day old wound on the back of SKH-1 hairless mice were infected with ~$1x10^9$ XEN 41 bioluminescent *P. aeruginosa* cells growing as biofilms to allow imaging of the infection using the In Vivo Imaging System.

2-day old biofilms were treated for 4-hrs using an agarose hydrogel imbedded with either triclosan or tobramycin alone or in combination. Triclosan hydrogels had no effect compared to control hydrogels while tobramycin hydrogels resulted in statistically non-significant 2.5-fold-reduction in bioluminescence (Fig. 6). Hydrogels embedded with triclosan and tobramycin resulted in statistically significant 4.5-fold-reduction in bioluminescence. The combination hydrogels resulted in greater than 4-fold reduction in five mice whereas tobramycin treatment only achieved this level of killing once.

## Discussion

Here we report that triclosan acts as a protonophore uncoupler against *P. aeruginosa* growing as biofilms (34-38). To our knowledge, this is the first report of protonophore activity by triclosan against Gram-negative bacteria growing as biofilms both *in vitro* and *in vivo*.

Adaptive resistance, occurring within 2-hrs of exposure, reduces accumulation of antimicrobials by inducing the activity of PMF driven RND-type efflux pumps and alterations to the OM (8-12) . We previously demonstrated classic aminoglycoside adaptive resistance, finding *P. aeruginosa* biofilms were refractory to tobramycin killing until ~6-hrs, with the greatest resistance observed at 2-hrs. However, the addition of triclosan with tobramycin led to rapid killing of *P. aeruginosa* biofilms (28). Here we show that triclosan reduces the activity of PMF driven RND-type efflux pumps, resulting in greater tobramycin accumulation within cells (Figs. 3 and 4). Triclosan does this by inhibiting a tobramycin induced surge in $\Delta\psi$ occurring at 2-hrs (Fig. 5). Together, our past and present data suggest that the disruption of the $\Delta\psi$ depletes the energy required for effective efflux pump mediated adaptive resistance (Fig. 7) (28). In support of this model, methyl-triclosan, which lacks a dissociable proton and thus cannot act as

protonophore, was completely ineffective alone and in combination with tobramycin (Figs. S3-5).

In addition to protein-specific corruption of translation at ribosomes, the very process of aminoglycoside uptake augments its bactericidal activity by non-specifically disrupting the OM and IM (18-20). In the first step of uptake, positively charged aminoglycosides bind to the negative charged components of the OM, including lipopolysaccharide and phospholipids in Gram-negative bacteria. This is followed by the displacement of magnesium ions responsible for OM stabilization, promoting uptake by disrupting and increasing OM permeability (18-20). In addition, aminoglycosides can diffuse through porins in the OM (18-20). In EDP-I, aminoglycosides cross the IM via a mechanism that is influenced by the PMF, specifically the $\Delta\psi$, in a concentration dependent manner (18-20). In EDP-II, aminoglycoside cause the mistranslation of proteins by membrane associated ribosomes, resulting in the insertion of misfolded proteins in the IM, which permeabilizes the cytoplasmic membrane accelerating its own accumulation (18-20).

Several studies have shown that aminoglycoside-mediated killing of bacteria can be enhanced by supplementing exogenous metabolites or host derived molecules, which increase cellular respiration, PMF, and the uptake of aminoglycosides through EDP-I (57-62). However, these studies used aminoglycoside concentrations ranging from 2-25 μg/mL on cells growing planktonically (57-62). Alternatively, the experiments described here used 250 μg/mL of tobramycin on *P. aeruginosa* biofilms. This higher concentration of tobramycin is more clinically relevant and similar to antipseudomonal therapeutic dosing in cystic fibrosis patients (1-3, 21, 22).

Although our model might appear to contradict these prior studies, it has been demonstrated that at concentrations of aminoglycosides greater than 30 μg/mL, as used here, the PMF is less important for aminoglycoside uptake during EDP-I (18-20). In fact, we observed that 250 μg/mL tobramycin can ultimately lead to biofilm killing at 24-hrs similar to the combination, suggesting that slow uptake of tobramycin during the EDP-I phase in the absence of triclosan eventually permeabilizes the IM stimulating EDP-II uptake in most of the biofilm (Fig. S7) (4, 48). However, the addition of triclosan accelerates this process by uncoupling the PMF such that maximal killing occurs at 4-hrs, as previously described (Fig. S7) (28). Together, our results support a model where triclosan reduction of the $\Delta\psi$ reduces the PMF required for active efflux leading to rapid accumulation of tobramycin in the cytoplasm and the stimulation of EDP-II uptake, which triggers irreversible cytosolic tobramycin accumulation and cell killing (4). In support of our model, other publications have demonstrated that bacteria can be sensitized to antibiotics by molecules that dissipate the PMF (24-27, 63-66). Specifically, Verstraeten et al., found that depleting the $\Delta\psi$ by overexpressing Obg in *E. coli* increased intercellular accumulation of tobramycin, likely through reduced efflux (65).

RND-type efflux pumps are intricately linked to antibiotic resistance, especially in biofilms (4, 54, 67). RND-type efflux pumps consist of three proteins which span the inner membrane and outer membrane (Fig. 7) (54). The inner membrane protein (IMP, e.g. MexX) catalyzes the $H^+$ dependent efflux of compounds and provides antimicrobial specificity whereas the periplasmic membrane fusion protein (MFP, e.g. MexY) connects the outer membrane protein (OMP, e.g. OprM) to the IMP creating an exit channel (54). There are 12 RND-type efflux pumps encoded in the genome of *P. aeruginosa* (4) and five are well characterized: MexAB-OprM, MexCD-OprJ, MexEF-OprN, MexXY-OprM and MexJK-OpRM (4). In

361 particular, the MexXY-OprM pump is responsible for aminoglycoside efflux, playing an
362 essential role in adaptive and acquired resistance (9-12, 68). The most frequent class of
363 aminoglycoside resistant mutants in CF isolates of *P. aeruginosa* have lost function of the
364 repressor MexZ, leading to overproduction of the RND-type efflux pump MexXY (67, 69). We
365 previously demonstrated that the combination of tobramycin and triclosan exhibited significant
366 killing against a clinical CF *P. aeruginosa* isolate AMT0023_34 that is tobramycin resistant by
367 such a mechanism (28). Importantly, our results suggest that the triclosan addition can potentiate
368 tobramycin to treat *P. aeruginosa* infections that are tobramycin resistant due to the
369 overexpression of efflux pumps. Which of the multiple efflux pumps impacted by triclosan
370 addition is under investigation.

371 We show that triclosan reduces efflux pump activity through the reduction of the $\Delta\psi$, but
372 this activity does not potentiate the cells to triclosan itself, even though the RND-type efflux
373 pump TriABC is a triclosan resistance mechanism expressed by *P. aeruginosa* (31). We
374 hypothesize that although triclosan reduces efflux pump activity, this reduction is not sufficient
375 to render *P. aeruginosa* sensitive to triclosan because this species also encodes the triclosan
376 resistant FabI ortholog FabV (30). In addition, if triclosan reduces efflux pump activity, one may
377 predict it should broadly enhance multiple classes of antibiotics (70). However, our prior study
378 demonstrated that triclosan only enhanced aminoglycosides and to a lesser extent, tetracycline
379 (28). Because triclosan does not completely abolish the $\Delta\psi$, we hypothesize that triclosan only
380 enhances antibiotic killing by bacteria that are known to trigger adaptive resistance through
381 disrupting translation, such as aminoglycosides and tetracyclines (8-10, 12-15).

382 *P. aeruginosa* encodes two genes for elongation factor G (EF-G), *fusA1* and *fusA2* (71).
383 *In vitro* translation studies have suggested that *fusA2* is the primary EF-G responsible for

ribosome translocation while the function of *fusA1* remains unclear (71). *fusA1* and *fusA2* are 98% similar and 84% identical, but interestingly *fusA1* expression is induced in cells growing as biofilms compared to cells growing planktonically (72). Recently, a new tobramycin resistance mechanism caused by mutations in *fusA1* has been identified in CF *P. aeruginosa* isolates (73). In fact, one of the mutations that we report here, L40Q, was identified in clinical isolates (73). These results support our findings that mutations in *fusA1* reduce susceptibility to aminoglycosides through an unknown mechanism(s).

In addition to mutations in the gene *fusA1*, all resistant mutants had SNPs or deletions in the previously described genes *ptsP*, involved in the overproduction of the phenazine pyocyanin responsible for the generation of reactive oxygen species (74), *mexT*, a repressor of the RND-type efflux pump MexEF-OprN (75), and *wspF*, a regulatory of the diguanylate cyclase WspR (76-78) (Table 1). Mutations in *mexT* were deletions or the SNP P170L (Table 1). These mutations and deletions likely result in the overexpression of the RND-type efflux pump MexEF-OprN due to loss of repression by MexT (75). This finding supports our model that the inhibition of efflux pump activity by triclosan drives increased tobramycin accumulation and activity. It is unclear what benefits would be provided by increased pyocyanin production, a quorum sensing controlled metabolite that is toxic and plays numerous roles in *P. aeruginosa* physiology and virulence (79). There is evidence to suggest pyocyanin may restrict social cheating in biofilms and promote tolerance to oxidative stress, which may provide some tolerance to tobramycin and triclosan treatment (80). Mutations in *wspF* are not surprising as these promote the formation of highly tolerant biofilms by increasing intracellular cyclic di-GMP stimulating increased EPS production that reduces the diffusion of tobramycin (76-78).

Owing to decades of overuse, the FDA has restricted the use of triclosan due to concerns over bioaccumulation and the potential for induction of resistance to other antibiotics in bacteria. However, triclosan maintains FDA approval for use in Colgate® total toothpaste at 100-times the concentrations used in this study. In support of this decision, numerous toxicity studies and the Scientific Committee on Consumer Safety published by the European Union has found that triclosan is safe when used appropriately (40-42). Furthermore, envisioning triclosan as an adjuvant for tobramycin therapy for CF, we previously performed acute and long-term triclosan toxicity studies in rats and showed that direct delivery of triclosan to lungs did not elicit significant toxicity (28).

More broadly, our results suggest that protonophores could be potent antibiotic adjuvants that enhance antibiotic killing against bacterial biofilms. Protonophores are being developed as novel antibiotics to target *Mtb*. Specifically, diphenyl ethers such as SQ109 are in phase II clinical trials in humans (24-27, 64). Moreover, a HTS recently identified that the c-Jun N-terminal kinase inhibitor SU3327, renamed halicin, dissipates the ΔpH and PMF, demonstrating growth inhibitory properties both *in vitro* and *in vivo* against several pathogens including some multi-drug resistant strains (66). Importantly, protonophore uncouplers are already routinely used for parasitic infections, including oxyclozanide, which we previously found synergizes with tobramycin much like triclosan (39). In addition to protonophores functioning as antimicrobials, there is also renewed interest in using these compounds to target such diseases as diabetes and cancer, as well as slow aging, suggesting compounds with this activity are druggable targets when used appropriately (81-83). Together, our results and other published studies demonstrate that the use of protonophore uncouplers to target bacterial energetics is a promising new strategy to target antimicrobial resistant infections (24).

## Methods

### Bacterial strains, culture conditions, and compounds.

All strains used in this study are listed in Table 1. Bacterial strains were grown in glass test tubes (18 X 150 mm) at 35ºC in cation adjusted Müeller-Hinton Broth II (MHB, Sigma-Aldrich) with agitation at 210 revolutions per minute (RPM). Antibiotics, methyl-triclosan, carbonyl cyanide 3-chlorophenylhydrazone (CCCP), and triclosan were obtained from Sigma-Aldrich. AFN-1252 was obtained from MedChemExpress. Tobramycin sulfate, gentamicin sulfate, and streptomycin sulfate were dissolved in autoclaved deionized water and filter sterilized using 0.22 µM filter membranes (Thomas Scientific). Triclosan was dissolved in 100% ethanol. Methyl-triclosan, CCCP, and AFN-1252 were dissolved in 100% dimethyl sulfoxide (DMSO).

### Biofilm susceptibility testing using BacTiter-Glo™.

To measure the antimicrobial susceptibility of biofilms, the MBEC Assay® (Innovotech) was used as described (28). Briefly, an overnight culture was diluted and seeded into a MBEC plate in 10% MHB v/v diluted in DPBS and incubated for 24-hrs at 35ºC with agitation at 150 RPM. The MBEC lid was then washed to remove non-adherent cells, transferred to a 96-well treatment plate, and incubated for the indicated time at 35ºC without agitation. Following treatment, the MBEC lid was washed and transferred to a black 96-well ViewPlate (PerkinElmer) filled with 40% (v/v) BacTiter-Glo™ (Promega) diluted in DPBS to enumerate cell viability using luminescence by an EnVison Multilabel Plate Reader (PerkenElmer, Waltham, MA). The BacTiter-Glo™ Microbial Cell Viability Assay is a luminescent assay that determines the

number of viable cells based on quantification of ATP concentration. A calibration curve was previously performed and it was found using a linear regression the coefficient of determination was $r^2$=0.9884 for luminescence versus CFUs/mL (28).

**Selection for *P. aeruginosa* resistant mutants.**

To select mutants resistant to tobramycin and triclosan, we modified a protocol by Lindsey and collages and serially passaged biofilms while treating them with ever increasing concentrations of triclosan and tobramycin (Table S1) (44). 24-hr biofilms were formed as described above and treated with triclosan and tobramycin for 24-hrs. After each treatment, biofilms were sonicated for 15-mins (Branson Ultrasonics) to disperse surviving cells from the pegs into 10% v/v MHB recovery media. Biofilms were then allowed to re-form on new pegs overnight. The next day, passaged biofilms were treated at a slightly higher concentration of triclosan and tobramycin. Following the treatment, the recovery process was repeated, and biofilms were re-formed. We split the treatment groups into three regimens: gradual, moderate and sudden (Table S1). The gradual treatment group was initially treated with 0.4 µM of triclosan and 0.004 µM of tobramycin, which is 250x less than the MIC of tobramycin (28). The moderate treatment group was initially treated with 8 µM of triclosan and 0.08 µM of tobramycin, which is 12.5x less than the MIC of tobramycin (28). And then the two treatment groups were treated in subsequent cycles with ever increasing concentrations of triclosan and tobramycin at the same rate. The sudden treatment series was treated with 500 µM of triclosan and tobramycin from cycle day 1 and was eradicated. By serially passaging biofilms and gradually increasing the concentration of triclosan and tobramycin, two resistant mutant populations were established, 30_B2 and 30_F1 (Cycle_Location on 96-well plate). Each mutant

pool was then streaked on LB agar plates for single colony isolation, and 96 single colony mutants were isolated from each plate, totaling 192 single colony mutants.

**Whole genome sequencing.**

Genomic deoxyribonucleic acid (gDNA) was isolated from each mutant using the Wizard® gDNA purification kit (Promega). Illumina NextSeq was then performed by the Genomic Services Facility at Indiana University Center for Genomics and Bioinformatics. To identify single nucleotide polymorphisms (SNPs), sequencing results were first verified for quality using FASTQC and aligned to the PAO1 reference genome (84), which can be downloaded from the *Pseudomonas* Genome Database (http://www.pseudomonas.com) using the *Breseq* pipeline, which can be downloaded from (http://barricklab.org) (85). All identified SNPs are listed in the supplemental spreadsheet.

**Ethidium bromide efflux pump assay.**

Intercellular accumulation of ethidium bromide, which is a substrate for RND-type efflux pumps, was measured fluorometrically as previously described (49, 86). As described above, 24-hr old biofilms were formed in 96-well black ViewPlate. 10 µg/mL of ethidium bromide was added to each well along with various treatments. Fluorescence was recorded every 2-hrs for 6-hrs using a SpectraMax M5 microplate spectrophotometer system ($\lambda_{excite}/\lambda_{emit}$ 530/600 nm).

**BacLight™ membrane potential assay and cell permeabilization assay.**

To measure changes in membrane potential and cellular permeabilization the BacLight™ Membrane Potential Assay was used in combination with the cell impermeable live/dead TO-Pro™-3 iodide stain, as previously described (39). Briefly, 24-hr old biofilms were formed in glass test tubes (18 x 150 mm) in 1 mL of 10% (v/v) MHB at 35°C and agitated at 150 RPM. Cells were washed in DPBS to remove non-adherent cells and treated with triclosan and tobramycin for 2-hrs. Following treatment, cells were washed in DPBS (without magnesium and calcium), and the biofilm was disrupted from the air-liquid interface. The cells were stained in 1 mL of DPBS for 5-mins with DiOC2(3). This dye emits in the fluorescein isothiocyanate (FITC) channel within all cells. However, greater membrane potential drives accumulation and stacking of the dye in the cell cytoplasm, shifting emission to the phycoerythrin (PE) channel. TO-PRO™-3 iodide, which emits in the allophycocyanin (APC) channel, was used to identify permeabilized cells, which fluoresces in cells that have compromised membranes by intercalating DNA. Single cell flow cytometry was performed on an LSR II (BD Biosciences), with excitation from 488 mm and 640 mm lasers, and analyzed in FITC/PE and APC channels, respectively.

**Tobramycin accumulation and extrusion assay.**

To measure the accumulation of tobramycin within cells in biofilms, tobramycin was conjugated to Texas red (Sigma-Aldrich) using an amine conjugation reaction, as previously described (50). Briefly, one milligram of Texas Red sulfonyl chloride (Thermo Fisher Scientific) was resuspended in 50 μL of anhydrous N,N-dimethylformamide (Sigma-Aldrich) on ice. The

solution was added slowly to 2.3 mL of 100 mM K2CO3 at pH 8.5, with or without 10 mg/mL tobramycin (Sigma-Aldrich), on ice. Conjugated tobramycin was used at a concentration of 250 µg/mL (~500 µM) alone and in combination with 100 µM of triclosan against 24-hr old biofilms formed in glass test tubes at the air-liquid interface, as described above. Following treatments, biofilms were washed in DPBS and then disrupted with autoclaved wooden sticks into 1 mL of 0.2% Triton X-100 to lyse cells (Sigma-Aldrich). Lysed cells were then transferred to spectrophotometer cuvettes (Thermo Fisher Scientific) and read using a SpectraMax M5 microplate spectrophotometer system ($\lambda_{excite}/\lambda_{emit}$ 595/615 nm). Extrusion assays were performed in a similar fashion, except after 30-mins of treatment, biofilms were washed three times in DPBS and then allowed to recover in treatment-free 1% MHB media for 30-mins. After recovery, the media was read as described above.

**DPBS-starved *P. aeruginosa* biofilms.**

24-hr old biofilms were formed on MBEC™ plates as described above. After 24-hrs, the lid was washed for 5-mins to remove non-adherent cells, transferred to a 96-well plate containing DPBS, and incubated at 35ºC with agitation at 150 RPM for 5-days.

**Agarose hydrogels.**

Agarose hydrogels were made as previously described (56). Briefly, by dissolving 1 gm of agarose (Sigma-Aldrich) into 200 mL of Tris-acetate-EDTA (TAE) buffer and heated to form a homogenous solution using a microwave. The 0.5% agarose solution was then allowed to cool and various treatments were added. The solution was then poured into 100 x 15 mm petri dishes

(Thermo Fisher Scientific) and stored at 4°C overnight. Prior to treatment, a 4 mm biopsy punch (VWR) was used to create hydrogel wafers.

**Murine wound infection model.**

Wound surgery was performed on 8-9 week-old male and female SKH-1 mice (Charles River) and infected with a bioluminescent derivative of PAO1, Xen41 (PerkinElmer), which constitutively expresses *luxCDABE* gene, as previously described with the following modifications (55, 56). Briefly, 24-hr old biofilms were formed on sterilized polycarbonate membrane filters with a 0.2 µM pore size (Millipore Sigma) by diluting an overnight culture to an $OD_{600}$ of 0.001 and pipetting 100 µl on 4 membranes on a tryptic soy agar (TSA) plate. 24-hr old biofilms were scrapped using L-shaped spreaders (Sigma-Aldrich) from each membrane and re-suspended in 500 µl of DPBS. 20 µl of the biofilm-suspension was inoculated into the 24-hr old wounds previously formed on the dorsal side of the mouse midway between the head and the base of the tail. 24-hrs later the biofilm within the wound was imaged using *in vivo* imaging system (IVIS) (Perkin Elmer). Then the biofilm was treated by placing a 4 mm 0.5% agarose hydrogel wafer either containing various treatments or only being made up of agarose alone on top of the wound. To quantify antimicrobial activity, the wound was then imaged 4-hrs later using IVIS and total flux (p/s) in radiance was used to quantify bacterial susceptibility. The loss of radiance indicates fewer cells are present within the wound. Vertebrate research was approved by the Michigan State University Institutional Animal Care and Use Committee application 03/18-036-00.

## Statistics

Significance was determined as described in accompanying figure legends by either a one-way ANOVA or two-way ANOVA followed by Sidak's or Bonferroni's multiple comparisons posttest, respectively. Unpaired t-test were also used as described in accompanying figure legends. The "n" indicates the number of biological replicates. For murine wound infection experiments, sample sizes were determined based on preliminary studies using groups that were sufficient to achieve a desired power of 0.85 and an alpha value of 0.05. All analyses were performed using GraphPad Prism version 8.4.1 (San Diego, CA) and a $p$-value of $< 0.05$ was considered statistically significant.

## Acknowledgments

This work was supported by grants from the Hunt for a Cure Foundation, the NSF BEACON center for evolution in action (DBI-0939454), NIH grants GM109259, GM110444, and AI143098 to C.M.W. and the Cystic Fibrosis Foundation Traineeship to M.M.M. In addition, M.M.M. was supported by a Wentworth Fellowship and Rudolf Hugh award from the MSU Department of Microbiology and Molecular Genetics and by a Dissertation Completion Fellowship from the College of National Science. We thank both Sandra O'Reilly and Louis King of the Michigan State Research Technology Support Facility for their assistance in the wound model and flow cytometry experiments, respectively. We also thank the Genomic Services Facility at Indiana University Center for Genomics and Bioinformatics. And we thank Lucas Demey, Mitchell Zachos and Emily Horning for their technical assistance.

**Table**

**Table 1. Bacterial strains used in this study.**

| Strain | Characteristics | Reference |
|---|---|---|
| PAO1 | *P. aeruginosa* Standard Reference Strain | (28) |
| Xen41 | Bioluminescent PAO1 derivative:<br>constitutively expresses *luxCDABE* gene | PerkinElmer |
| 30_F1_5 | *fusA1*, L40Q (C**T**G→C**A**G)<br>*wspF*, Q132* (CAG→TAG)<br>*PtsP*, A718P (**G**CC→**C**CC)<br>*mexT*, P170L (C**C**G→C**T**G) | This Study |
| 30_F1_6 | *fusA1*, L40Q (C**T**G→C**A**G)<br>*wspF*, Q132* (CAG→TAG)<br>*PtsP*, coding (703/2280 nt)<br>*mexT*, coding (58-137/1044 nt) | This Study |
| 30_B2_8 | *fusA1*, T64A (**A**CC→**G**CC)<br>*wspF*, Q132* (CAG→TAG)<br>*PtsP*, coding (703/2280 nt)<br>*mexT*, coding (58-137/1044 nt) | This Study |
| 30_B2_30 | *fusA1*, T64A (**A**CC→**G**CC)<br>*wspF*, Q132* (CAG→TAG)<br>*PtsP*, A718P (**G**CC→**C**CC)<br>*mexT*, P170L (C**C**G→C**T**G) | This Study |
| 30_B2_57 | *fusA1*, T64A (**A**CC→**G**CC)<br>*wspF*, Q132* (CAG→TAG)<br>*PtsP*, coding (703/2280 nt)<br>*mexT*, coding (58-137/1044 nt) | This Study |
| 30_B2_82 | *fusA1*, T64A (**A**CC→**G**CC)<br>*wspF*, Q132* (CAG→TAG)<br>*PtsP*, A718P (**G**CC→**C**CC)<br>*mexT*, P170L (C**C**G→C**T**G) | This Study |

All additional SNPs in evolution mutants are listed in the supplemental spreadsheet.

## Figure legends

**FIG 1. Triclosan in combination with tobramycin results in increased permeabilization of cells within biofilms.** 24-hr old biofilms were treated with triclosan (100 µM), or tobramycin (500 µM), alone and in combination for 2-hrs. Cells were stained with the live/dead cell indicator TO-PRO™-3 iodide to determine the number of cells that were permeabilized. The results are percent averages plus the standard error mean (SEM, n=4). Percent values indicate the average relative abundance of events within each gate normalized to the total number of events analyzed, excluding artifacts, aggregates and debris. A one-way analysis of variance (ANOVA) followed by Sidak's multiple comparison post-hoc test was used to determine statistical significance between each treatment and the untreated control or tobramycin treatment alone with the combination treatment. *, $p<0.05$. NS, not significant.

**FIG 2. Mutants from experimental evolution are resistant to tobramycin and the combination.** 24-hr old biofilms were treated with triclosan (100 µM) and tobramycin (500 µM) alone and in combination. The results represent the means plus SEM (n=6). A two-way ANOVA followed by Bonferroni's posttest was used to determine statistical significance between each treatment and the untreated control. *, $p<0.05$. NS, not significant.

**FIG 3. Triclosan reduces the activity of RND-type efflux pumps.** 24-hr biofilms were stained with ethidium bromide to measure accumulation. Biofilms were treated with CCCP (100 µM), triclosan (100 µM), tobramycin (500 µM) alone and in combination. Fluorescence was read at 0,2,4, and 6-hrs. Results represent the average arbitrary fluorescence units ±SEM (n=6).

**FIG 4. Triclosan results in increased cellular accumulation and extrusion of Texas Red conjugated tobramycin (TbTR).** 24-hr old biofilms grown in glass test tubes were treated for 30-mins with triclosan (100 µM), CCCP (100 µM) and TbTR (250 µg/mL). (A) Then cells were disrupted from the biofilms and lysed with 0.2% Triton-X 100® to measure intercellular accumulation of TbTR. (B) To measure extrusion, biofilms were first treated for 30-mins and washed three-times in DPBS. Biofilms then recovered in treatment free media for 30-mins and fluorescence of the media was measured. TbTR was measured by relative fluorescence units using excitation $595_{nm}$ and emission $615_{nm}$. Results represent the average arbitrary fluorescence units ±SEM (n=6). For panel A, a One-Way-ANOVA was performed comparing TbTR alone vs CCCP and TbTR and vs triclosan and TbTR. For panel B, an unpaired t-test was performed comparing TbTR versus triclosan and TbTR. *, $p<0.05$. NS, not significant.

**FIG 5. Triclosan reduces the membrane potential surge induced by tobramycin at 2-hours.** 24-hr old biofilms were treated with triclosan (100 µM), or tobramycin (500 µM), alone and in combination for 2-hrs. Cells were stained with DiOC2(3) to measure the membrane potential. Dead or permeabilized cells were excluded from membrane potential analysis by parallel staining with the dead cell indicator TO-PRO™-3 iodide. The results are percent averages plus the SEM (n=4). Percent values indicate the average relative abundance of events within each gate normalized to the total number of events analyzed, excluding dead cells, artifacts, aggregates and debris. A one-way ANOVA followed by Sidak's multiple comparison post-hoc test was used to determine statistical significance between each treatment and the untreated control, and tobramycin treatment alone was compared with the combination. *, $p<0.05$. NS, not significant.

**FIG 6. Triclosan and tobramycin hydrogels are more effective than tobramycin hydrogels in a murine wound model.** 24-hr old bioluminescent biofilms formed within wounds were treated with triclosan (100 µM), or tobramycin (400 µM), alone and in combination for 4-hrs in a hydrogel. Reduction in the number of cells within biofilms was quantified using IVIS. The results are fold reduction of three separate experiments ±SEM, no treatment n=6, triclosan n=6, tobramycin n=10, triclosan and tobramycin n=9. A one-way ANOVA followed by Bonferroni's multiple comparison post-hoc test was used to determine statistical significance between each treatment and the untreated control and tobramycin treatment alone was compared with tobramycin and triclosan (*, $p<0.05$).

**FIG 7. Triclosan sensitizes *P. aeruginosa* to tobramycin by acting as a protonophore, inhibiting efflux pump activity, and abolishing adaptive resistance.** (1) Within 2-hrs of exposure to tobramycin, adaptive resistance occurs, (2) which is due to the induction of RND-type efflux pumps and surge in membrane potential ($\Delta\psi$), resulting in reduced accumulation of tobramycin within the cytosol. (3) Triclosan shuttles protons across the inner membrane, collapsing the proton motive force ($\Delta p$) and depolarizing the $\Delta\psi$. Consequently, efflux pump activity is reduced and there is enhanced accumulation of tobramycin within the cytosol. Finally, tobramycin binds to the A-site of the ribosome, corrupting protein synthesis and causing membrane permeabilization. Overall, triclosan accelerates and increase the effectiveness of tobramycin by reducing the $\Delta\psi$ and efflux pump activity. Proton gradient, $\Delta pH$. Outer membrane protein (OMP), membrane fusion protein (MFP), inner membrane protein (IMP).

## Supplemental Figure Legends

**FIG S1. AFN-1252 alone or in combination with tobramycin is not effective against mature biofilms.** 24-hr old biofilms grown on MBEC plates were treated for 6-hrs with AFN-1252 (400 µM), tobramycin (400 µM), alone and in combination in two-fold dilutions, and the number of viable cells within the biofilms were quantified by BacTiter-Glo™. The assay was performed twice in in duplicate. The results represent means ± the Standard Error Mean (SEM). A one-way analysis of variance (ANOVA) followed by Bonferroni's multiple comparison post-hoc test was used to determine statistical significance between tobramycin versus the combination (NS, not significant).

**FIG S2. Initial tobramycin treatment is required for the combination to be effective.** 24-hr old biofilms grown on MBEC plates were treated sequentially. First, biofilms were treated for 3-hours with tobramycin (500 µM) and then washed three times in DPBS for 3-mins each, before being treated with triclosan (100 µM) for 3-hours or vice versa. As a control, biofilms were also treated for 6-hrs with triclosan and tobramycin. The number of viable cells within the biofilms were quantified by BacTiter-Glo™. The assay was performed twice in in duplicate. The results represent means plus the SEM. A one-way ANOVA followed by Bonferroni's multiple comparison post-hoc test was used to determine statistical significance between each treatment and the untreated control. *, $p<0.05$. NS, not significant.

**FIG S3. Methyl-triclosan alone or in combination with tobramycin is not effective against mature biofilms.** 24-hr old biofilms grown on MBEC plates were treated for 6-hrs with methyl-triclosan (100 µM), tobramycin (400 µM), alone and in combination in two-fold dilutions, and

the number of viable cells within the biofilms were quantified by BacTiter-Glo™. The assay was performed twice in in duplicate. The results represent means ±SEM. A one-way ANOVA followed by Bonferroni's multiple comparison post-hoc test was used to determine statistical significance compared to tobramycin alone and the combination. NS, not significant.

**FIG S4. Methyl-triclosan alone and in combination with tobramycin does not reduced the surge in membrane potential induced by tobramycin at 2-hours.** 24-hr old biofilms were treated with methyl-triclosan (100 µM), or tobramycin (500 µM), alone and in combination for 2-hrs. Cells were stained with DiOC2(3) and TO-PRO™-3 iodide to determine the number of cells that maintained a membrane potential (A) or were permeabilized (B), respectively. Dead or permeabilized cells were excluded from membrane potential analysis and are shown in panel B. The experiment was performed two separate times in duplicate. The results are percent averages plus the SEM. Percent values indicate the average relative abundance of events within each gate normalized to the total number of events analyzed, excluding artifacts, aggregates and debris. A one-way ANOVA followed by Sidak's multiple comparison post-hoc test was used to determine statistical significance between each treatment and an untreated control, and tobramycin treatment alone was compared with the combination. *, $p<0.05$, NS, not significant.

**FIG S5. Methyl-triclosan does not reduced RND-type efflux pump activity.** Ethidium bromide is a substrate of RND-type efflux pumps. 24-hr biofilms were stained with ethidium bromide to measure accumulation. Biofilms were treated with methyl-triclosan (100 µM) and tobramycin (500 µM) alone and in combination. Fluorescence was read at 0,2,4, and 6-hrs. The

assay was performed three times in triplicate. Results represent the average arbitrary fluorescence units ±SEM.

**FIG S6. DPBS starved biofilms are not more sensitive to tobramycin alone.** 24-hour old biofilms were starved of nutrients by replacing media with DPBS for 5-days. Starved biofilms were treated with triclosan (100 µM), or tobramycin (500 µM), alone and in combination for 6-hrs. The number of viable cells within the biofilms was quantified using the BacTiter-Glo™ assay. The assay was performed once using three biological replicates. The results represent the means plus the SEM. A one-way ANOVA followed by Sidak's multiple comparison post hoc test was used to determine statistical significance between the combination treatment and the untreated control and between triclosan alone or tobramycin alone and the combination treatment as indicated by the bars. *, $P < 0.05$.

**FIG S7. Tobramycin is as effective as the combination after 24-hrs of treatment.** 24-hr old biofilms were treated for 24-hrs with triclosan (100 µM), tobramycin (500 µM), alone and in combination, and the number of viable cells within the biofilms were quantified by BacTiter-Glo™. The assay was performed at least three times in triplicate. The results represent means plus the SEM. A one-way ANOVA followed by Bonferroni's multiple comparison post-hoc test was used to determine statistical significance between untreated biofilms, tobramycin alone, and the combination treatment. In addition, using the same analysis, a comparison was made between tobramycin alone and the combination treatment. *, $P < 0.05$. NS, not significant. 4-hr treatments were previously published and are shown for comparison (28).

**References:**

1. Donlan RM, Costerton JW. Biofilms: survival mechanisms of clinically relevant microorganisms. Clin Microbiol Rev. 2002;15(2):167-93.

2. O'Sullivan BP, Freedman SD. Cystic fibrosis. The Lancet. 2009;373(9678):1891-904.

3. Omar A, Wright JB, Schultz G, Burrell R, Nadworny P. Microbial Biofilms and Chronic Wounds. Microorganisms. 2017;5(1):9.

4. Poole K. *Pseudomonas aeruginosa*: resistance to the max. Front Microbiol. 2011;2:65.

5. Livermore DM. Penicillin-binding proteins, porins and outer-membrane permeability of carbenicillin-resistant and -susceptible strains of *Pseudomonas aeruginosa*. J Med Microbiol. 1984;18(2):261-70.

6. Morita Y, Tomida J, Kawamura Y. Responses of *Pseudomonas aeruginosa* to antimicrobials. Front Microbiol. 2014;4.

7. Barclay ML, Begg EJ, Chambers ST, Thornley PE, Pattemore PK, Grimwood K. Adaptive resistance to tobramycin in *Pseudomonas aeruginosa* lung infection in cystic fibrosis. J Antimicrob Chemother. 1996;37(6):1155-64.

8. Hay T, Fraud S, Lau CH, Gilmour C, Poole K. Antibiotic inducibility of the *mexXY* multidrug efflux operon of *Pseudomonas aeruginosa*: involvement of the MexZ anti-repressor ArmZ. PLoS One. 2013;8(2):e56858.

9. Jeannot K, Sobel ML, El Garch F, Poole K, Plesiat P. Induction of the MexXY efflux pump in *Pseudomonas aeruginosa* is dependent on drug-ribosome interaction. J Bacteriol. 2005;187(15):5341-6.

10. Hocquet D, Vogne C, El Garch F, Vejux A, Gotoh N, Lee A, et al. MexXY-OprM efflux pump is necessary for a adaptive resistance of *Pseudomonas aeruginosa* to aminoglycosides. Antimicrobial agents and chemotherapy. 2003;47(4):1371-5.

11. Karlowsky JA, Saunders MH, Harding GA, Hoban DJ, Zhanel GG. In vitro characterization of aminoglycoside adaptive resistance in *Pseudomonas aeruginosa*. Antimicrob Agents Chemother. 1996;40(6):1387-93.

12. Yamamoto M, Ueda A, Kudo M, Matsuo Y, Fukushima J, Nakae T, et al. Role of MexZ and PA5471 in transcriptional regulation of *mexXY* in *Pseudomonas aeruginosa*. Microbiology. 2009;155(Pt 10):3312-21.

13. Barclay ML, Begg EJ. Aminoglycoside adaptive resistance: importance for effective dosage regimens. Drugs. 2001;61(6):713-21.

14. Barclay ML, Begg EJ, Chambers ST. Adaptive resistance following single doses of gentamicin in a dynamic in vitro model. Antimicrob Agents Chemother. 1992;36(9):1951-7.

15. Barclay ML, Begg EJ, Chambers ST, Peddie BA. The effect of aminoglycoside-induced adaptive resistance on the antibacterial activity of other antibiotics against *Pseudomonas aeruginosa* in vitro. J Antimicrob Chemother. 1996;38(5):853-8.

16. Daikos GL, Lolans VT, Jackson GG. First-exposure adaptive resistance to aminoglycoside antibiotics in vivo with meaning for optimal clinical use. Antimicrob Agents Chemother. 1991;35(1):117-23.

17. Xiong YQ, Caillon J, Kergueris MF, Drugeon H, Baron D, Potel G, et al. Adaptive resistance of *Pseudomonas aeruginosa* induced by aminoglycosides and killing kinetics in a rabbit endocarditis model. Antimicrobial agents and chemotherapy. 1997;41(4):823-6.

18. Taber HW, Mueller JP, Miller PF, Arrow AS. Bacterial uptake of aminoglycoside antibiotics. Microbiol Rev. 1987;51(4):439-57.

19. Davis BD. Mechanism of bactericidal action of aminoglycosides. Microbiol Rev. 1987;51(3):341-50.

20. Hancock RE. Alterations in outer membrane permeability. Annu Rev Microbiol. 1984;38(1):237-64.

21. Mogayzel PJ, Jr., Naureckas ET, Robinson KA, Brady C, Guill M, Lahiri T, et al. Cystic Fibrosis Foundation pulmonary guideline. pharmacologic approaches to prevention and eradication of initial *Pseudomonas aeruginosa* infection. Ann Am Thorac Soc. 2014;11(10):1640-50.

22. Chmiel JF, Aksamit TR, Chotirmall SH, Dasenbrook EC, Elborn JS, LiPuma JJ, et al. Antibiotic management of lung infections in cystic fibrosis. I. The microbiome, methicillin-resistant *Staphylococcus aureus*, gram-negative bacteria, and multiple infections. Ann Am Thorac Soc. 2014;11(7):1120-9.

23. Brown ED, Wright GD. Antibacterial drug discovery in the resistance era. Nature. 2016;529(7586):336-43.

24. Hards K, Cook GM. Targeting bacterial energetics to produce new antimicrobials. Drug Resist Updat. 2018;36:1-12.

25. Andries K, Verhasselt P, Guillemont J, Gohlmann HW, Neefs JM, Winkler H, et al. A diarylquinoline drug active on the ATP synthase of *Mycobacterium tuberculosis*. Science. 2005;307(5707):223-7.

26. Hards K, Robson JR, Berney M, Shaw L, Bald D, Koul A, et al. Bactericidal mode of action of bedaquiline. J Antimicrob Chemother. 2015;70(7):2028-37.

27. Feng X, Zhu W, Schurig-Briccio LA, Lindert S, Shoen C, Hitchings R, et al. Antiinfectives targeting enzymes and the proton motive force. Proc Natl Acad Sci U S A. 2015;112(51):E7073-82.

28. Maiden MM, Hunt AMA, Zachos MP, Gibson JA, Hurwitz ME, Mulks MH, et al. Triclosan Is an Aminoglycoside Adjuvant for Eradication of *Pseudomonas aeruginosa* Biofilms. Antimicrob Agents Chemother. 2018;62(6):e00146-18.

29. Heath RJ, Rubin JR, Holland DR, Zhang E, Snow ME, Rock CO. Mechanism of triclosan inhibition of bacterial fatty acid synthesis. J Biol Chem. 1999;274(16):11110-4.

30. Zhu L, Lin J, Ma J, Cronan JE, Wang H. Triclosan resistance of *Pseudomonas aeruginosa* PAO1 is due to FabV, a triclosan-resistant enoyl-acyl carrier protein reductase. Antimicrob Agents Chemother. 2010;54(2):689-98.

31. Mima T, Joshi S, Gomez-Escalada M, Schweizer HP. Identification and characterization of TriABC-OpmH, a triclosan efflux pump of *Pseudomonas aeruginosa* requiring two membrane fusion proteins. J Bacteriol. 2007;189(21):7600-9.

32. Mitchell P. Coupling of phosphorylation to electron and hydrogen transfer by a chemi-osmotic type of mechanism. Nature. 1961;191(4784):144-8.

33. Mitchell P. Chemiosmotic coupling in oxidative and photosynthetic phosphorylation. 1966. Biochim Biophys Acta. 2011;1807(12):1507-38.

34. Yoon DS, Choi Y, Cha DS, Zhang P, Choi SM, Alfhili MA, et al. Triclosan Disrupts SKN-1/Nrf2-Mediated Oxidative Stress Response in C. elegans and Human Mesenchymal Stem Cells. Sci Rep. 2017;7(1):12592.

35. Weatherly LM, Shim J, Hashmi HN, Kennedy RH, Hess ST, Gosse JA. Antimicrobial agent triclosan is a proton ionophore uncoupler of mitochondria in living rat and human mast cells and in primary human keratinocytes. J Appl Toxicol. 2016;36(6):777-89.

36. Popova LB, Nosikova ES, Kotova EA, Tarasova EO, Nazarov PA, Khailova LS, et al. Protonophoric action of triclosan causes calcium efflux from mitochondria, plasma membrane depolarization and bursts of miniature end-plate potentials. Biochim Biophys Acta Biomembr. 2018;1860(5):1000-7.

37. Teplova VV, Belosludtsev KN, Kruglov AG. Mechanism of triclosan toxicity: Mitochondrial dysfunction including complex II inhibition, superoxide release and uncoupling of oxidative phosphorylation. Toxicol Lett. 2017;275:108-17.

38. Ajao C, Andersson MA, Teplova VV, Nagy S, Gahmberg CG, Andersson LC, et al. Mitochondrial toxicity of triclosan on mammalian cells. Toxicol Rep. 2015;2:624-37.

39. Maiden MM, Zachos MP, Waters CM. The ionophore oxyclozanide enhances tobramycin killing of *Pseudomonas aeruginosa* biofilms by permeabilizing cells and depolarizing the membrane potential. J Antimicrob Chemother. 2019;74(4):894-906.

40. Davison John SR, Maillard M, Pagès J-Y, Scenihr J-MO, et al. Scientific Committee on Consumer Safety (SCCS): Opinion on triclosan antimicrobial resistance. DG Sanco Scientific Committee on Consumer Safety. . 2010 22:1–56. .

41. Rodricks JV, Swenberg JA, Borzelleca JF, Maronpot RR, Shipp AM. Triclosan: a critical review of the experimental data and development of margins of safety for consumer products. Crit Rev Toxicol. 2010;40(5):422-84.

42. Fang JL, Stingley RL, Beland FA, Harrouk W, Lumpkins DL, Howard P. Occurrence, efficacy, metabolism, and toxicity of triclosan. J Environ Sci Health C Environ Carcinog Ecotoxicol Rev. 2010;28(3):147-71.

43. Rao KN, Lakshminarasimhan A, Joseph S, Lekshmi SU, Lau MS, Takhi M, et al. AFN-1252 is a potent inhibitor of enoyl-ACP reductase from *Burkholderia pseudomallei*--Crystal structure, mode of action, and biological activity. Protein Sci. 2015;24(5):832-40.

44. Lindsey HA, Gallie J, Taylor S, Kerr B. Evolutionary rescue from extinction is contingent on a lower rate of environmental change. Nature. 2013;494(7438):463-7.

45. Pal C, Papp B, Lazar V. Collateral sensitivity of antibiotic-resistant microbes. Trends Microbiol. 2015;23(7):401-7.

46. Rodnina MV, Savelsbergh A, Katunin VI, Wintermeyer W. Hydrolysis of GTP by elongation factor G drives tRNA movement on the ribosome. Nature. 1997;385(6611):37-41.

47. Arnaud Bolard PPs, and Katy Jeannota. Mutations in Gene fusA1 as a Novel Mechanism of Aminoglycoside Resistance in Clinical Strains of *Pseudomonas aeruginosa*. Antimicrobial Agents and Chemotherapy. 2018;62(2):e01835-17.

48. Tseng BS, Zhang W, Harrison JJ, Quach TP, Song JL, Penterman J, et al. The extracellular matrix protects *Pseudomonas aeruginosa* biofilms by limiting the penetration of tobramycin. Environ Microbiol. 2013;15(10):2865-78.

49. Blair JM, Piddock LJ. How to Measure Export via Bacterial Multidrug Resistance Efflux Pumps. mBio. 2016;7(4):e00840-16.

50. Sandoval R, Leiser J, Molitoris BA. Aminoglycoside antibiotics traffic to the Golgi complex in LLC-PK1 cells. J Am Soc Nephrol. 1998;9(2):167-74.

51. Booth IR. The Regulation of Intracellular pH in Bacteria. Chichester, UK: John Wiley & Sons, Ltd.; 2007. 19-37 p.

52. Campbell BD, Kadner RJ. Relation of aerobiosis and ionic strength to the uptake of dihydrostreptomycin in *Escherichia coli*. Biochim Biophys Acta. 1980;593(1):1-10.

53. Paulsen IT, Brown MH, Skurray RA. Proton-dependent multidrug efflux systems. Microbiol Rev. 1996;60(4):575-608.

54. Venter H, Mowla R, Ohene-Agyei T, Ma S. RND-type drug efflux pumps from Gram-negative bacteria: molecular mechanism and inhibition. Front Microbiol. 2015;6:377.

55. Agostinho Hunt AM, Gibson JA, Larrivee CL, O'Reilly S, Navitskaya S, Needle DB, et al. A bioluminescent *Pseudomonas aeruginosa* wound model reveals increased mortality of type 1 diabetic mice to biofilm infection. J Wound Care. 2017;26(Sup7):S24-S33.

56. Maiden MM, Zachos MP, Waters CM. Hydrogels Embedded With Melittin and Tobramycin Are Effective Against *Pseudomonas aeruginosa* Biofilms in an Animal Wound Model. Front Microbiol. 2019;10(1348):1348.

57. Allison KR, Brynildsen MP, Collins JJ. Metabolite-enabled eradication of bacterial persisters by aminoglycosides. Nature. 2011;473(7346):216-20.

58. Barraud N, Buson A, Jarolimek W, Rice SA. Mannitol enhances antibiotic sensitivity of persister bacteria in *Pseudomonas aeruginosa* biofilms. PLoS One. 2013;8(12):e84220.

59. Crabbe A, Ostyn L, Staelens S, Rigauts C, Risseeuw M, Dhaenens M, et al. Host metabolites stimulate the bacterial proton motive force to enhance the activity of aminoglycoside antibiotics. PLoS Pathog. 2019;15(4):e1007697.

60. Radlinski LC, Rowe SE, Brzozowski R, Wilkinson AD, Huang R, Eswara P, et al. Chemical Induction of Aminoglycoside Uptake Overcomes Antibiotic Tolerance and Resistance in *Staphylococcus aureus*. Cell Chem Biol. 2019;26(10):1355-64 e4.

61. Su YB, Peng B, Han Y, Li H, Peng XX. Fructose restores susceptibility of multidrug-resistant *Edwardsiella tarda* to kanamycin. J Proteome Res. 2015;14(3):1612-20.

62. Su YB, Peng B, Li H, Cheng ZX, Zhang TT, Zhu JX, et al. Pyruvate cycle increases aminoglycoside efficacy and provides respiratory energy in bacteria. Proc Natl Acad Sci U S A. 2018;115(7):E1578-E87.

63. Farha MA, Verschoor CP, Bowdish D, Brown ED. Collapsing the proton motive force to identify synergistic combinations against *Staphylococcus aureus*. Chem Biol. 2013;20(9):1168-78.

64. Foss MH, Pou S, Davidson PM, Dunaj JL, Winter RW, Pou S, et al. Diphenylether-Modified 1,2-Diamines with Improved Drug Properties for Development against *Mycobacterium tuberculosis*. ACS Infect Dis. 2016;2(7):500-8.

65. Verstraeten N, Knapen WJ, Kint CI, Liebens V, Van den Bergh B, Dewachter L, et al. Obg and Membrane Depolarization Are Part of a Microbial Bet-Hedging Strategy that Leads to Antibiotic Tolerance. Mol Cell. 2015;59(1):9-21.

66. Stokes JM, Yang K, Swanson K, Jin W, Cubillos-Ruiz A, Donghia NM, et al. A Deep Learning Approach to Antibiotic Discovery. Cell. 2020;180(4):688-702 e13.

67. Piddock LJ. Clinically relevant chromosomally encoded multidrug resistance efflux pumps in bacteria. Clin Microbiol Rev. 2006;19(2):382-402.

68. Morita Y, Tomida J, Kawamura Y. MexXY multidrug efflux system of *Pseudomonas aeruginosa*. Front Microbiol. 2012;3(408):408.

69. Mena A, Smith EE, Burns JL, Speert DP, Moskowitz SM, Perez JL, et al. Genetic adaptation of *Pseudomonas aeruginosa* to the airways of cystic fibrosis patients is catalyzed by hypermutation. J Bacteriol. 2008;190(24):7910-7.

70. Askoura M, Mottawea W, Abujamel T, Taher I. Efflux pump inhibitors (EPIs) as new antimicrobial agents against *Pseudomonas aeruginosa*. Libyan J Med. 2011;6.

71. Palmer SO, Rangel EY, Hu Y, Tran AT, Bullard JM. Two homologous EF-G proteins from *Pseudomonas aeruginosa* exhibit distinct functions. PLoS One. 2013;8(11):e80252.

72. Anderson GG, Moreau-Marquis S, Stanton BA, O'Toole GA. In vitro analysis of tobramycin-treated *Pseudomonas aeruginosa* biofilms on cystic fibrosis-derived airway epithelial cells. Infect Immun. 2008;76(4):1423-33.

73. Bolard A, Plesiat P, Jeannot K. Mutations in Gene fusA1 as a Novel Mechanism of Aminoglycoside Resistance in Clinical Strains of *Pseudomonas aeruginosa*. Antimicrob Agents Chemother. 2018;62(2).

74. Xu H, Lin W, Xia H, Xu S, Li Y, Yao H, et al. Influence of ptsP gene on pyocyanin production in *Pseudomonas aeruginosa*. FEMS Microbiol Lett. 2005;253(1):103-9.

75. Juarez P, Broutin I, Bordi C, Plesiat P, Llanes C. Constitutive Activation of MexT by Amino Acid Substitutions Results in MexEF-OprN Overproduction in Clinical Isolates of *Pseudomonas aeruginosa*. Antimicrob Agents Chemother. 2018;62(5).

76. D'Argenio DA, Calfee MW, Rainey PB, Pesci EC. Autolysis and autoaggregation in *Pseudomonas aeruginosa* colony morphology mutants. J Bacteriol. 2002;184(23):6481-9.

77. Hickman JW, Tifrea DF, Harwood CS. A chemosensory system that regulates biofilm formation through modulation of cyclic diguanylate levels. Proc Natl Acad Sci U S A. 2005;102(40):14422-7.

78. Starkey M, Hickman JH, Ma L, Zhang N, De Long S, Hinz A, et al. *Pseudomonas aeruginosa* rugose small-colony variants have adaptations that likely promote persistence in the cystic fibrosis lung. J Bacteriol. 2009;191(11):3492-503.

79. Lau GW, Hassett DJ, Ran H, Kong F. The role of pyocyanin in *Pseudomonas aeruginosa* infection. Trends Mol Med. 2004;10(12):599-606.

80. Castaneda-Tamez P, Ramirez-Peris J, Perez-Velazquez J, Kuttler C, Jalalimanesh A, Saucedo-Mora MA, et al. Pyocyanin Restricts Social Cheating in *Pseudomonas aeruginosa*. Front Microbiol. 2018;9(1348):1348.

81. Barbosa EJ, Lobenberg R, de Araujo GLB, Bou-Chacra NA. Niclosamide repositioning for treating cancer: Challenges and nano-based drug delivery opportunities. Eur J Pharm Biopharm. 2019;141:58-69.

82. Chen W, Mook RA, Jr., Premont RT, Wang J. Niclosamide: Beyond an antihelminthic drug. Cell Signal. 2018;41:89-96.

83. Childress ES, Alexopoulos SJ, Hoehn KL, Santos WL. Small Molecule Mitochondrial Uncouplers and Their Therapeutic Potential. J Med Chem. 2018;61(11):4641-55.

84. Winsor GL, Griffiths EJ, Lo R, Dhillon BK, Shay JA, Brinkman FS. Enhanced annotations and features for comparing thousands of *Pseudomonas* genomes in the *Pseudomonas* genome database. Nucleic Acids Res. 2016;44(D1):D646-53.

85. Deatherage DE, Barrick JE. Identification of mutations in laboratory-evolved microbes from next-generation sequencing data using breseq. Methods Mol Biol. 2014;1151:165-88.

86. Olmsted J, 3rd, Kearns DR. Mechanism of ethidium bromide fluorescence enhancement on binding to nucleic acids. Biochemistry. 1977;16(16):3647-54.

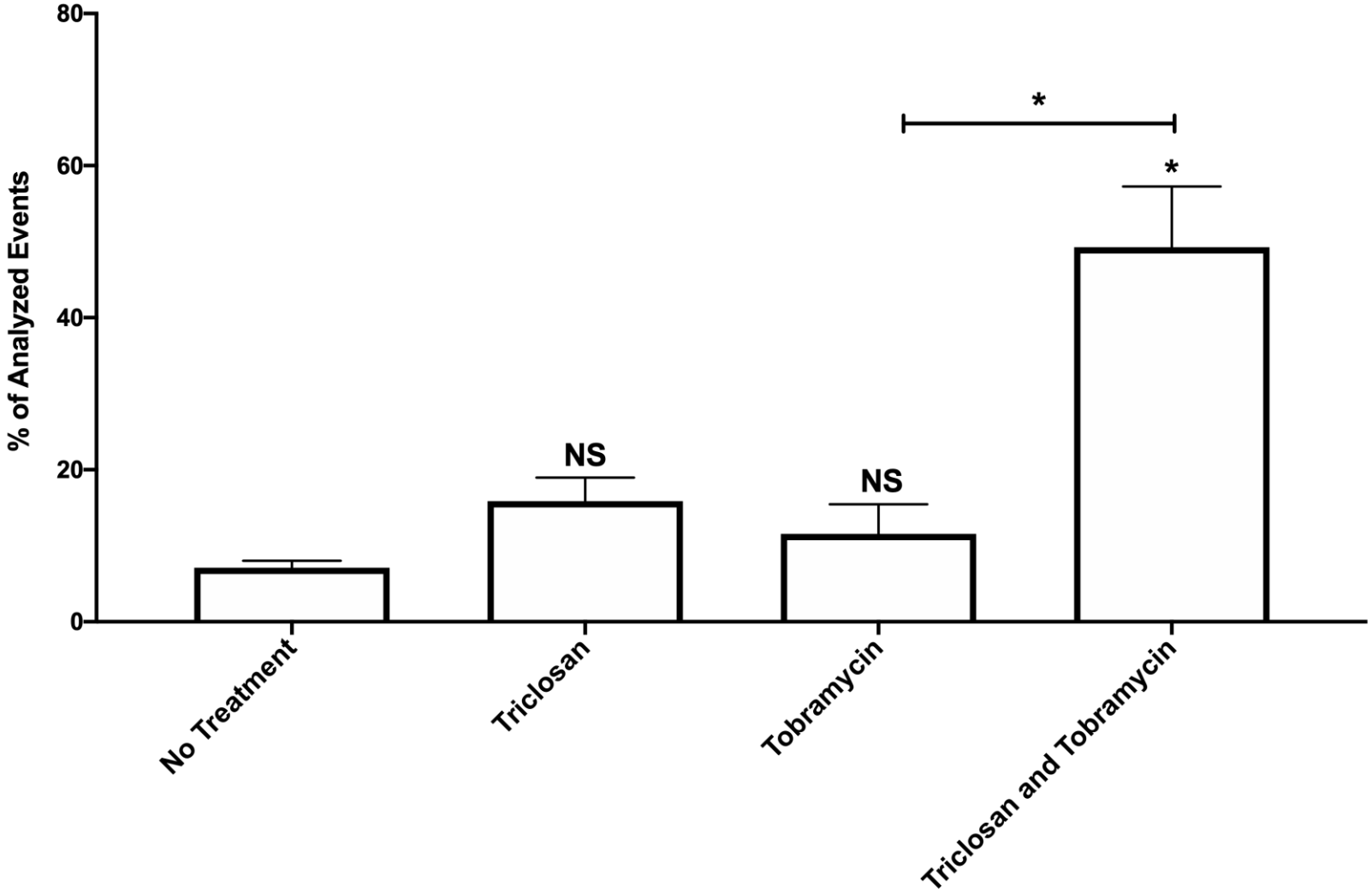


**FIG 1. Triclosan in combination with tobramycin results in increased permeabilization of cells within biofilms.** 24-hr old biofilms were treated with triclosan (100 µM), or tobramycin (500 µM), alone and in combination for 2-hrs. Cells were stained with the live/dead cell indicator TO-PRO™-3 iodide to determine the number of cells that were permeabilized. The results are percent averages plus the standard error mean (SEM, n=4). Percent values indicate the average relative abundance of events within each gate normalized to the total number of events analyzed, excluding artifacts, aggregates and debris. A one-way analysis of variance (ANOVA) followed by Sidak's multiple comparison post-hoc test was used to determine statistical significance between each treatment and the untreated control or tobramycin treatment alone with the combination treatment. *, $p<0.05$. NS, not significant.

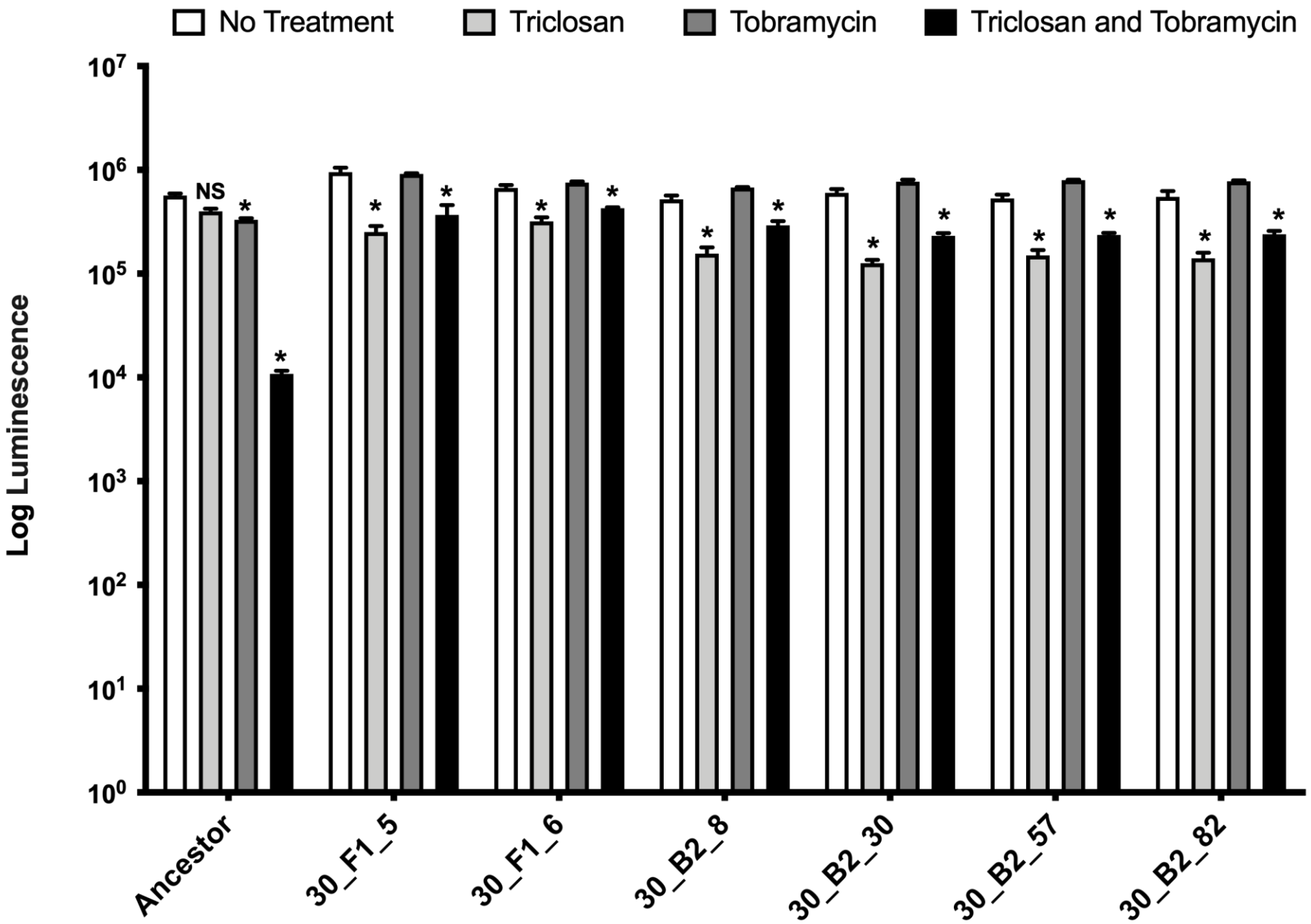


**FIG 2. Mutants from experimental evolution are resistant to tobramycin and the combination.** 24-hr old biofilms were treated with triclosan (100 µM) and tobramycin (500 µM) alone and in combination. The results represent the means plus SEM (n=6). A two-way ANOVA followed by Bonferroni's posttest was used to determine statistical significance between each treatment and the untreated control. *, $p<0.05$. NS, not significant.

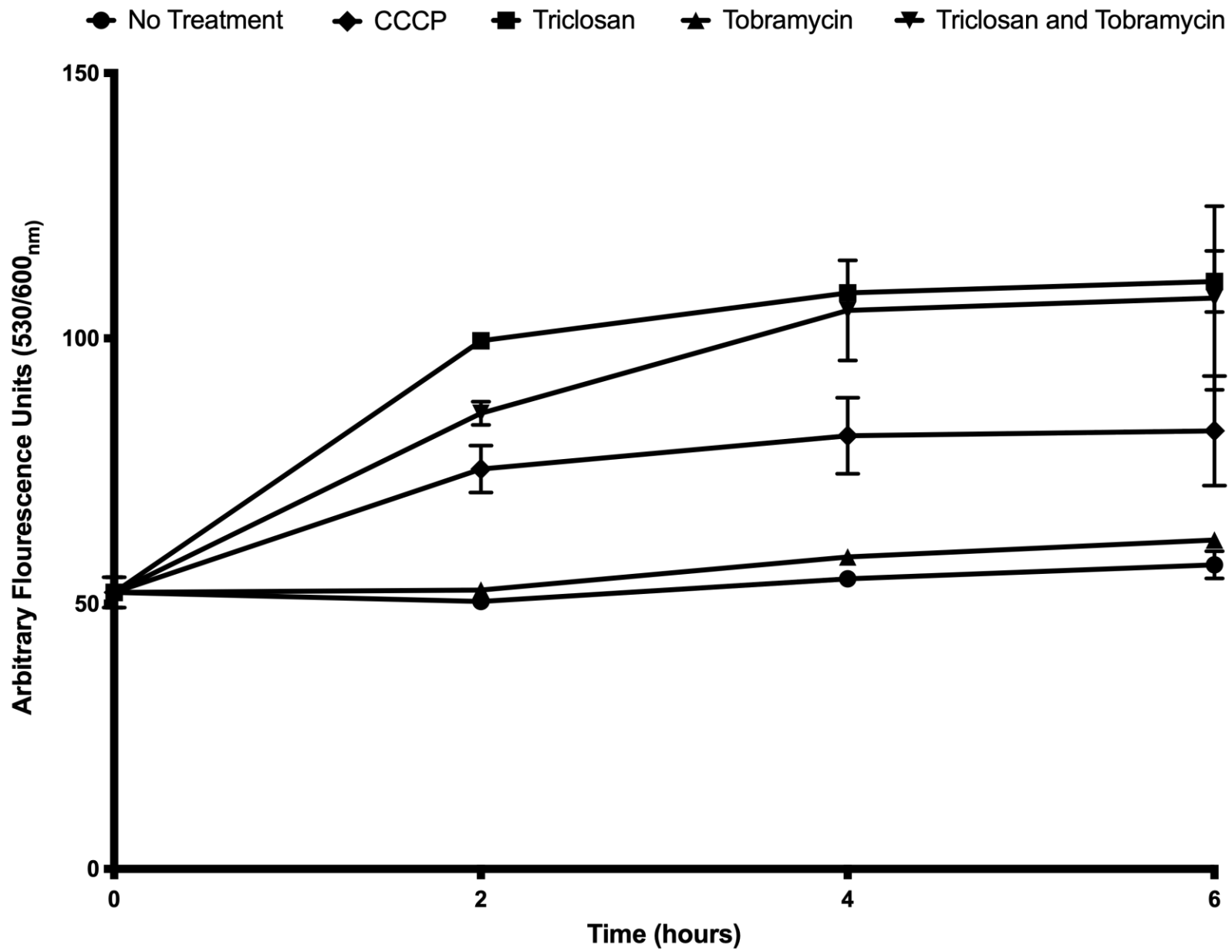


**FIG 3. Triclosan reduces the activity of RND-type efflux pumps.** 24-hr biofilms were stained with ethidium bromide to measure accumulation. Biofilms were treated with CCCP (100 µM), triclosan (100 µM), tobramycin (500 µM) alone and in combination. Fluorescence was read at 0,2,4, and 6-hrs. Results represent the average arbitrary fluorescence units ±SEM (n=6).

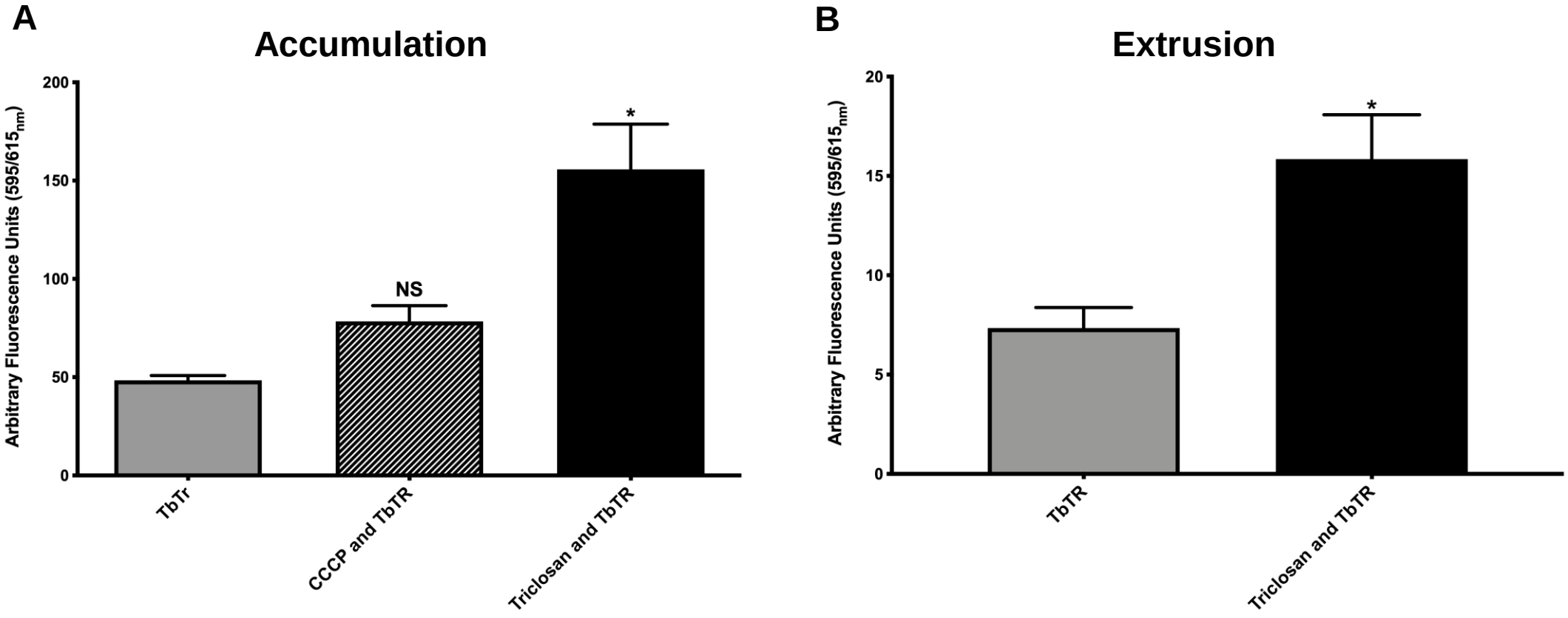


**FIG 4. Triclosan results in increased cellular accumulation and extrusion of Texas Red conjugated tobramycin (TbTR).** 24-hr old biofilms grown in glass test tubes were treated for 30-mins with triclosan (100 µM), CCCP (100 µM) and TbTR (250 µg/mL). (A) Then cells were disrupted from the biofilms and lysed with 0.2% Triton-X 100® to measure intercellular accumulation of TbTR. (B) To measure extrusion, biofilms were first treated for 30-mins and washed three-times in DPBS. Biofilms then recovered in treatment free media for 30-mins and fluorescence of the media was measured. TbTR was measured by relative fluorescence units using excitation $595_{nm}$ and emission $615_{nm}$. Results represent the average arbitrary fluorescence units ±SEM (n=6). For panel A, a One-Way-ANOVA was performed comparing TbTR alone vs CCCP and TbTR and vs triclosan and TbTR. For panel B, an unpaired t-test was performed comparing TbTR versus triclosan and TbTR. *, $p<0.05$. NS, not significant.

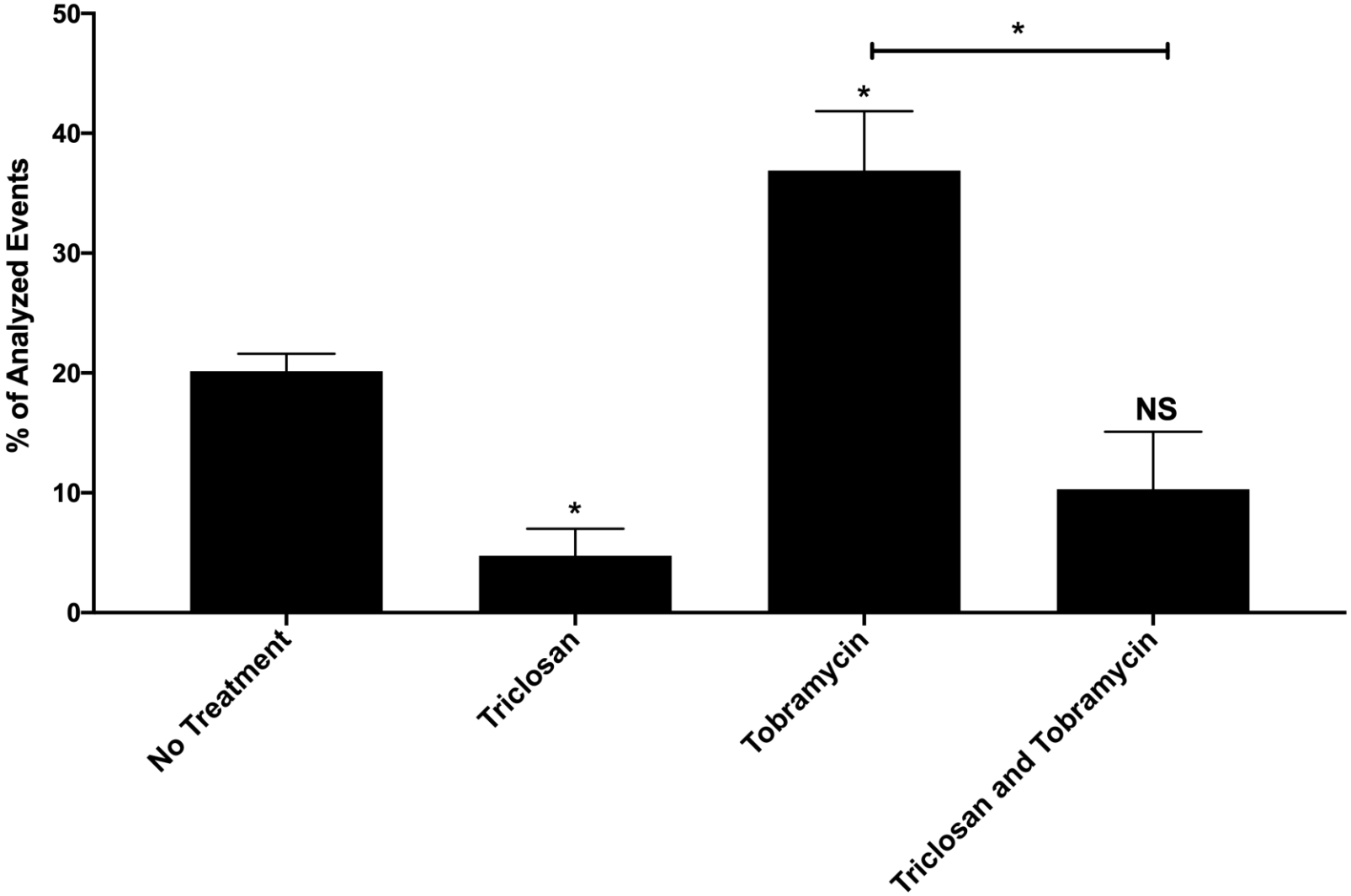


**FIG 5. Triclosan reduces the membrane potential surge induced by tobramycin at 2-hours.** 24-hr old biofilms were treated with triclosan (100 µM), or tobramycin (500 µM), alone and in combination for 2-hrs. Cells were stained with DiOC2(3) to measure the membrane potential. Dead or permeabilized cells were excluded from membrane potential analysis by parallel staining with the dead cell indicator TO-PRO™-3 iodide. The results are percent averages plus the SEM (n=4). Percent values indicate the average relative abundance of events within each gate normalized to the total number of events analyzed, excluding dead cells, artifacts, aggregates and debris. A one-way ANOVA followed by Sidak's multiple comparison post-hoc test was used to determine statistical significance between each treatment and the untreated control, and tobramycin treatment alone was compared with the combination. *, $p<0.05$. NS, not significant.

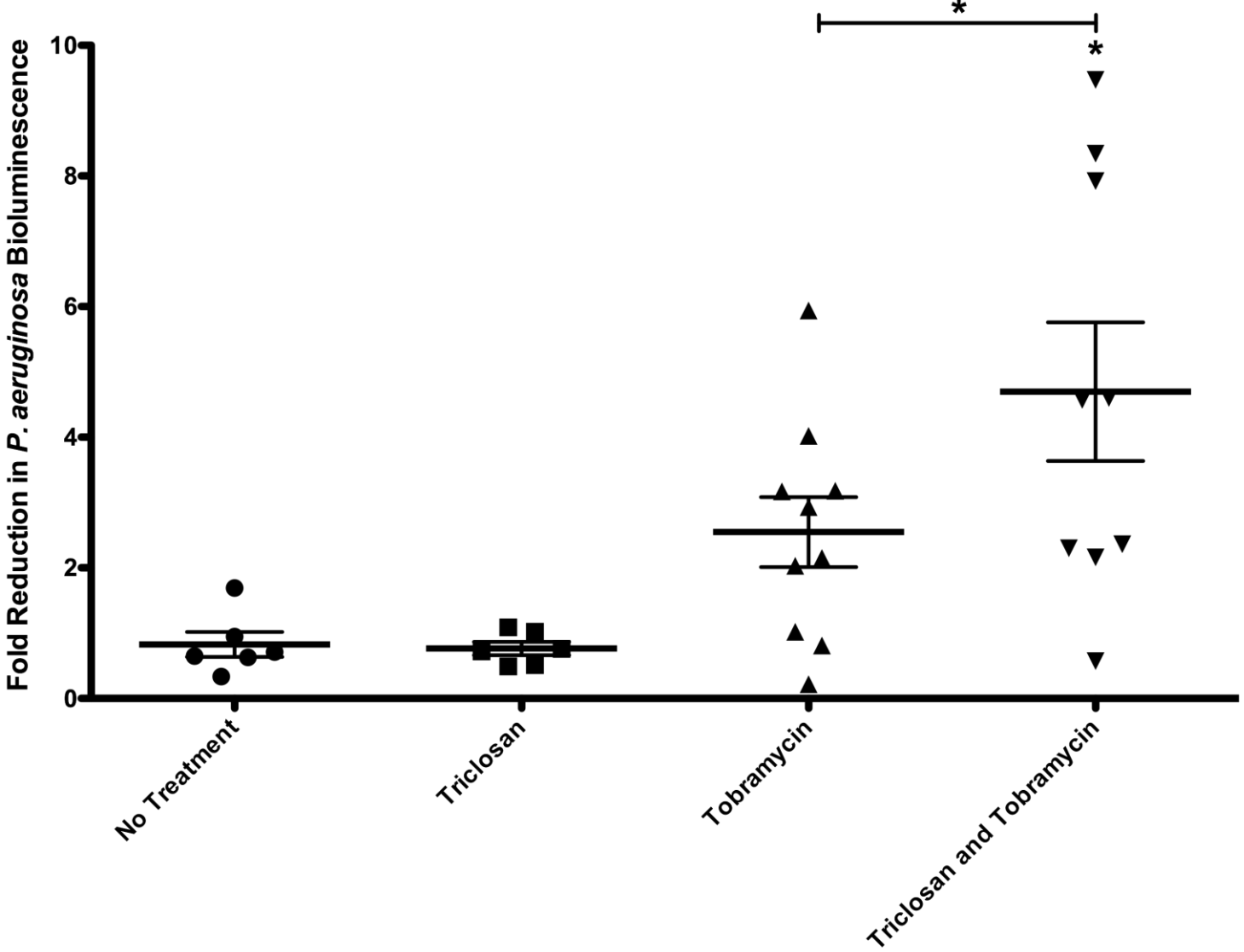


**FIG 6. Triclosan and tobramycin hydrogels are more effective than tobramycin hydrogels in a murine wound model.** 24-hr old bioluminescent biofilms formed within wounds were treated with triclosan (100 µM), or tobramycin (400 µM), alone and in combination for 4-hrs in a hydrogel. Reduction in the number of cells within biofilms was quantified using IVIS. The results are fold reduction of three separate experiments ±SEM, no treatment n=6, triclosan n=6, tobramycin n=10, triclosan and tobramycin n=9. A one-way ANOVA followed by Bonferroni's multiple comparison post-hoc test was used to determine statistical significance between each treatment and the untreated control and tobramycin treatment alone was compared with tobramycin and triclosan (*, $p<0.05$).

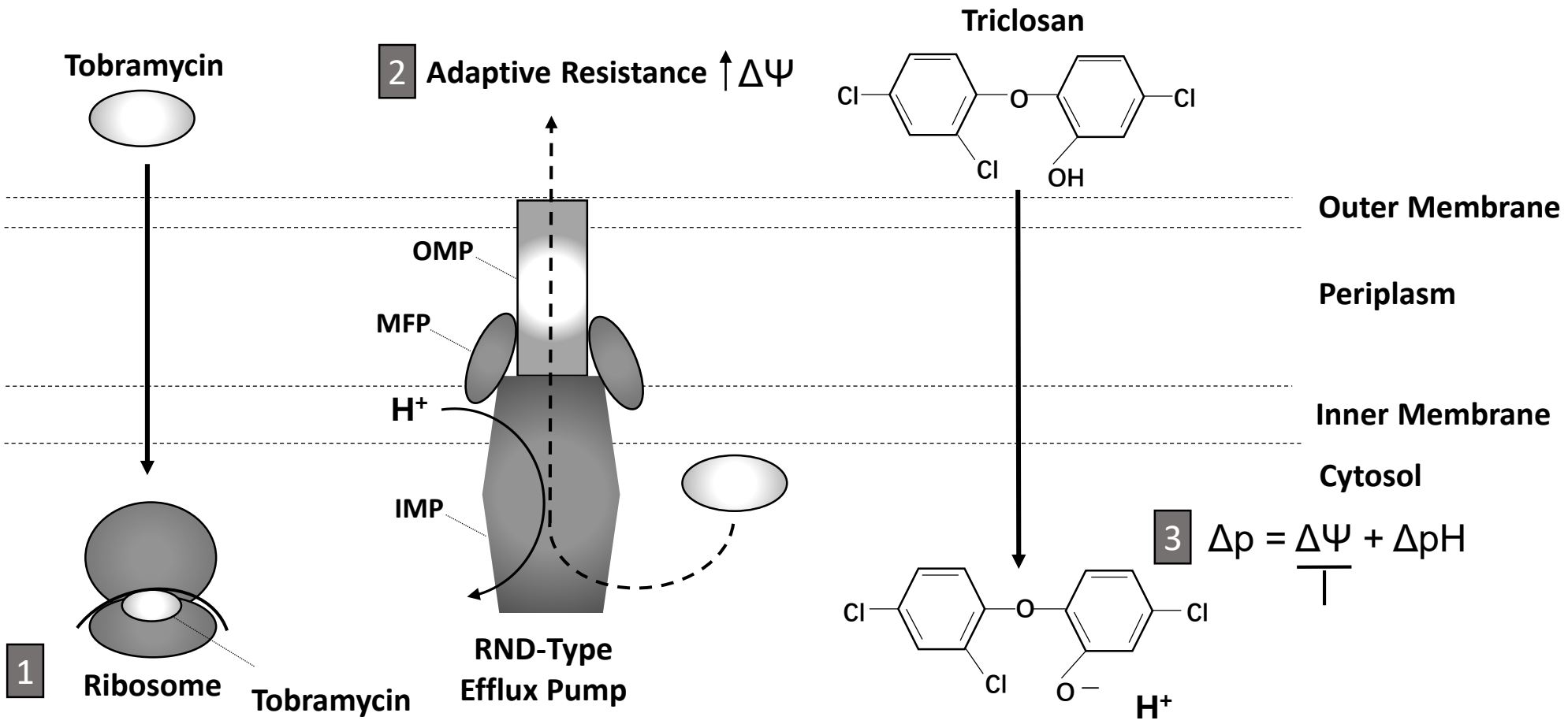


**FIG 7. Triclosan sensitizes *P. aeruginosa* to tobramycin by acting as a protonophore, inhibiting efflux pump activity, and abolishing adaptive resistance.** (1) Within 2-hrs of exposure to tobramycin, adaptive resistance occurs, (2) which is due to the induction of RND-type efflux pumps and surge in membrane potential (Δψ), resulting in reduced accumulation of tobramycin within the cytosol. (3) Triclosan shuttles protons across the inner membrane, collapsing the proton motive force (Δp) and depolarizing the Δψ. Consequently, efflux pump activity is reduced and there is enhanced accumulation of tobramycin within the cytosol. Finally, tobramycin binds to the A-site of the ribosome, corrupting protein synthesis and causing membrane permeabilization. Overall, triclosan accelerates and increase the effectiveness of tobramycin by reducing the Δψ and efflux pump activity. Proton gradient, ΔpH. Outer membrane protein (OMP), membrane fusion protein (MFP), inner membrane protein (IMP).

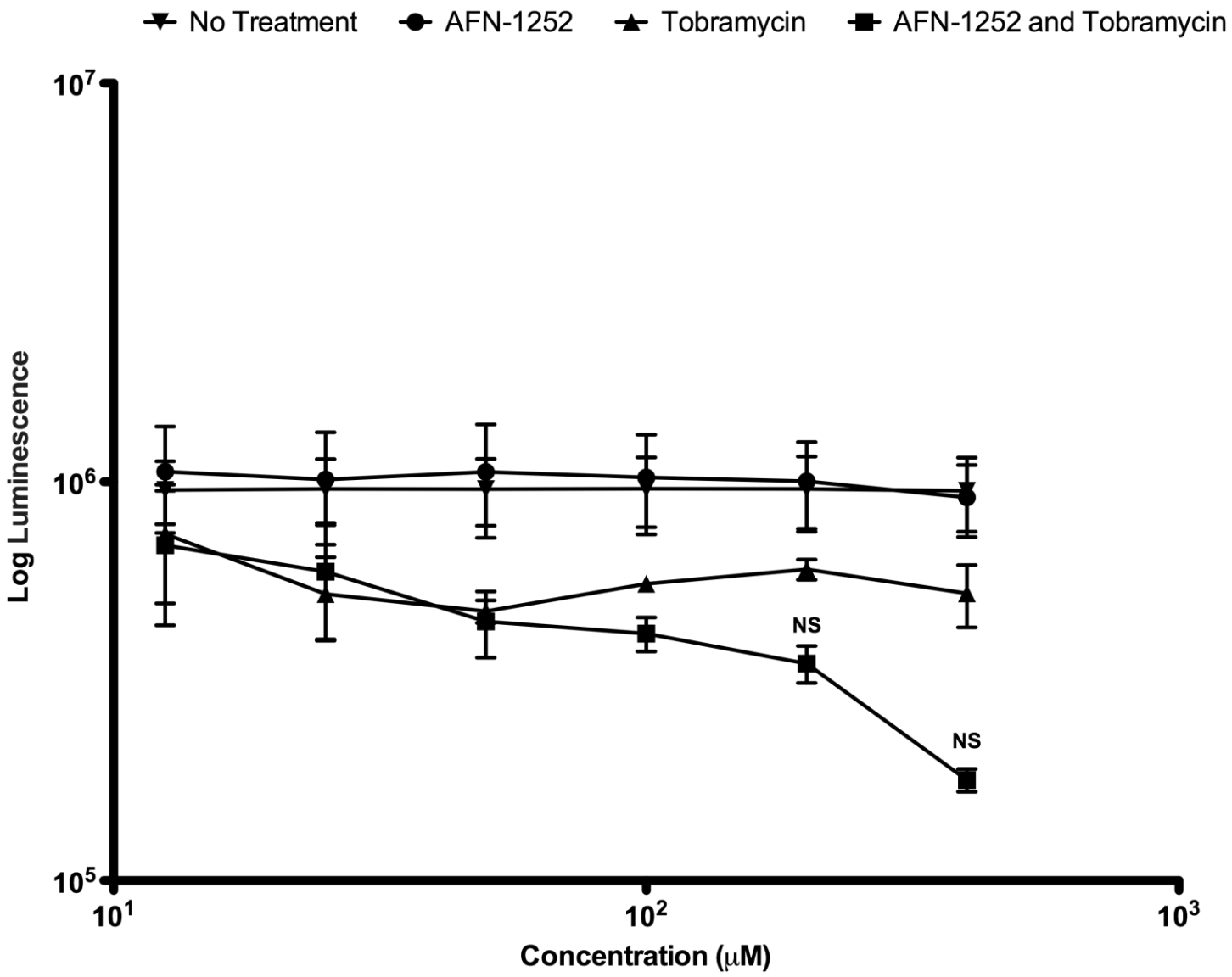


**FIG S1. AFN-1252 alone or in combination with tobramycin is not effective against mature biofilms.** 24-hr old biofilms grown on MBEC plates were treated for 6-hrs with AFN-1252 (400 µM), tobramycin (400 µM), alone and in combination in two-fold dilutions, and the number of viable cells within the biofilms were quantified by BacTiter-Glo™. The assay was performed twice in in duplicate. The results represent means ± the Standard Error Mean (SEM). A one-way analysis of variance (ANOVA) followed by Bonferroni's multiple comparison post-hoc test was used to determine statistical significance between tobramycin versus the combination (NS, not significant).

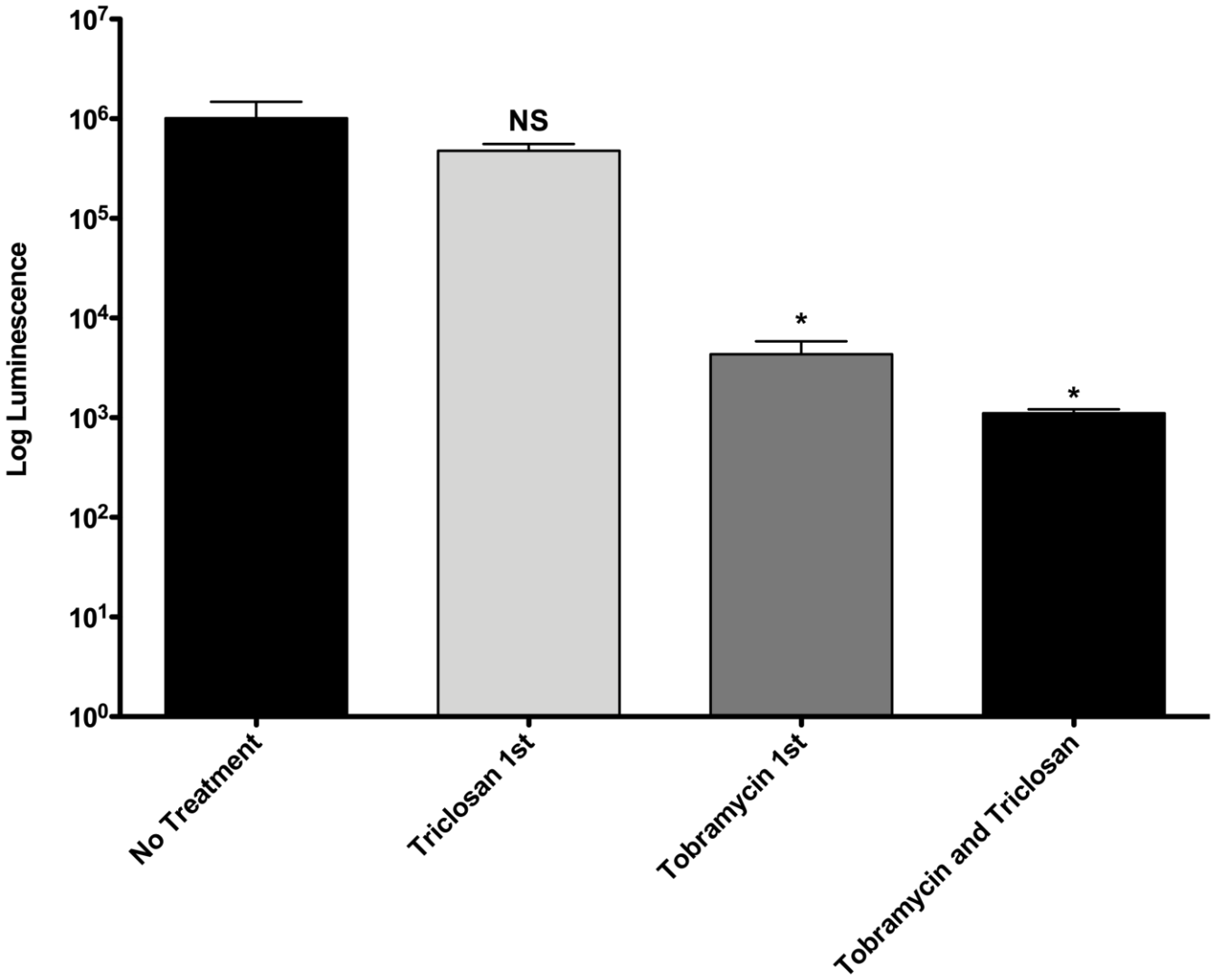


**FIG S2. Initial tobramycin treatment is required for the combination to be effective.** 24-hr old biofilms grown on MBEC plates were treated sequentially. First, biofilms were treated for 3-hours with tobramycin (500 µM) and then washed three times in DPBS for 3-mins each, before being treated with triclosan (100 µM) for 3-hours or vice versa. As a control, biofilms were also treated for 6-hrs with triclosan and tobramycin. The number of viable cells within the biofilms were quantified by BacTiter-Glo™. The assay was performed twice in in duplicate. The results represent means plus the SEM. A one-way ANOVA followed by Bonferroni's multiple comparison post-hoc test was used to determine statistical significance between each treatment and the untreated control. *, $p<0.05$. NS, not significant.

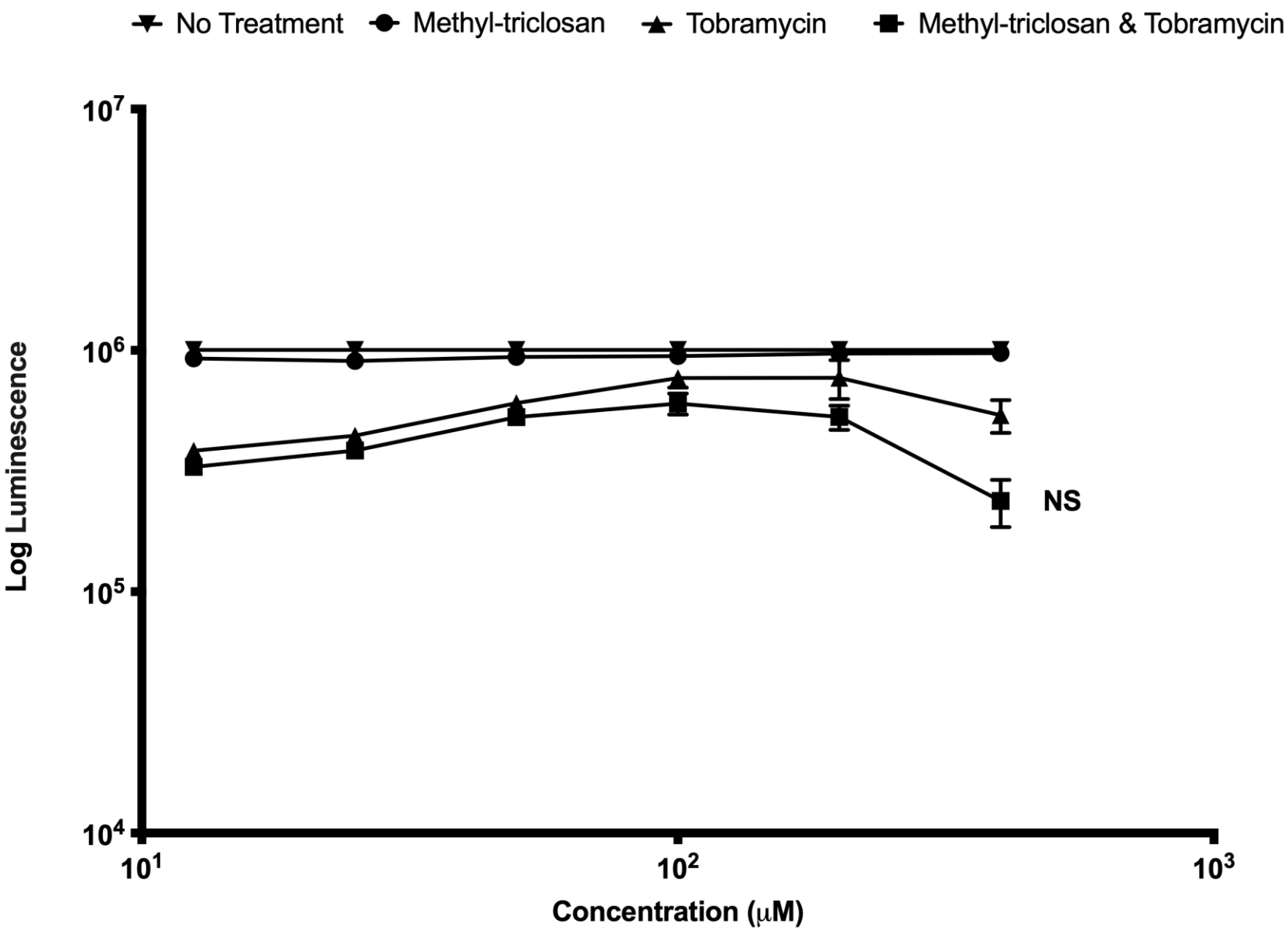


**FIG S3. Methyl-triclosan alone or in combination with tobramycin is not effective against mature biofilms.** 24-hr old biofilms grown on MBEC plates were treated for 6-hrs with methyl-triclosan (100 μM), tobramycin (400 μM), alone and in combination in two-fold dilutions, and the number of viable cells within the biofilms were quantified by BacTiter-Glo™. The assay was performed twice in in duplicate. The results represent means ±SEM. A one-way ANOVA followed by Bonferroni's multiple comparison post-hoc test was used to determine statistical significance compared to tobramycin alone and the combination. NS, not significant.

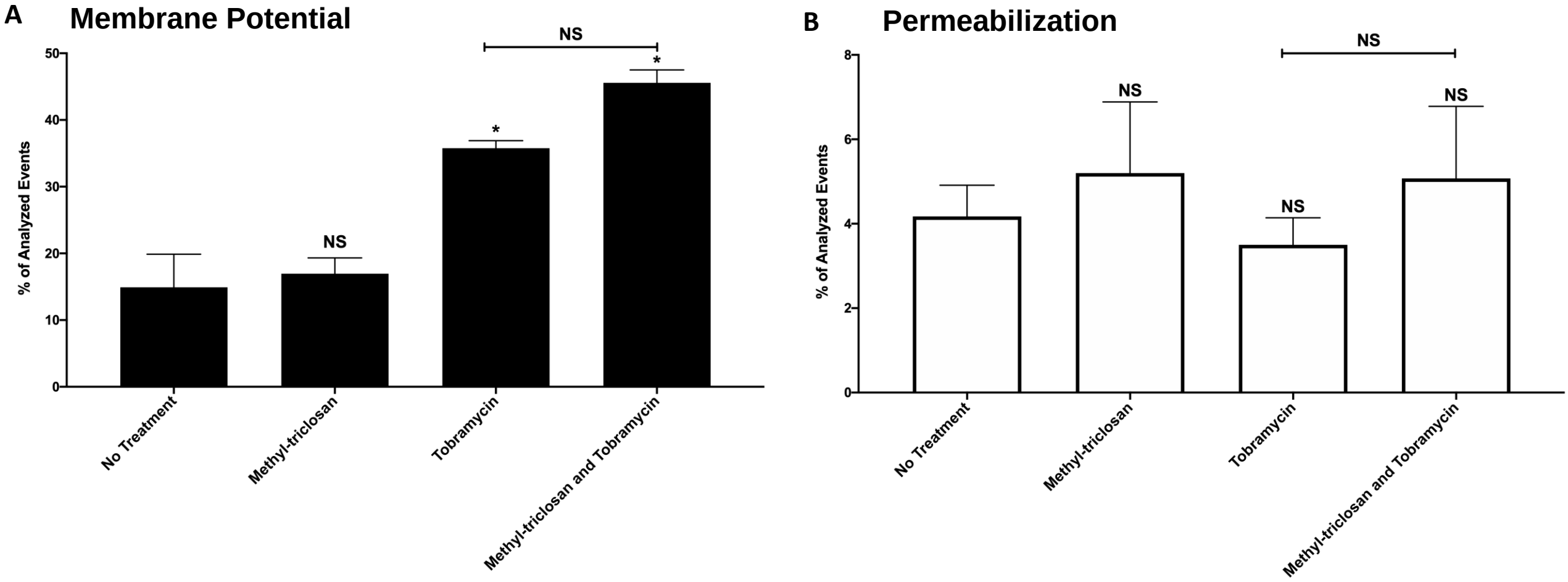


**FIG S4. Methyl-triclosan alone and in combination with tobramycin does not reduced the surge in membrane potential induced by tobramycin at 2-hours.** 24-hr old biofilms were treated with methyl-triclosan (100 µM), or tobramycin (500 µM), alone and in combination for 2-hrs. Cells were stained with DiOC2(3) and TO-PRO™-3 iodide to determine the number of cells that maintained a membrane potential (A) or were permeabilized (B), respectively. Dead or permeabilized cells were excluded from membrane potential analysis and are shown in panel B. The experiment was performed two separate times in duplicate. The results are percent averages plus the SEM. Percent values indicate the average relative abundance of events within each gate normalized to the total number of events analyzed, excluding artifacts, aggregates and debris. A one-way ANOVA followed by Sidak's multiple comparison post-hoc test was used to determine statistical significance between each treatment and an untreated control, and tobramycin treatment alone was compared with the combination. *, $p<0.05$, NS, not significant.

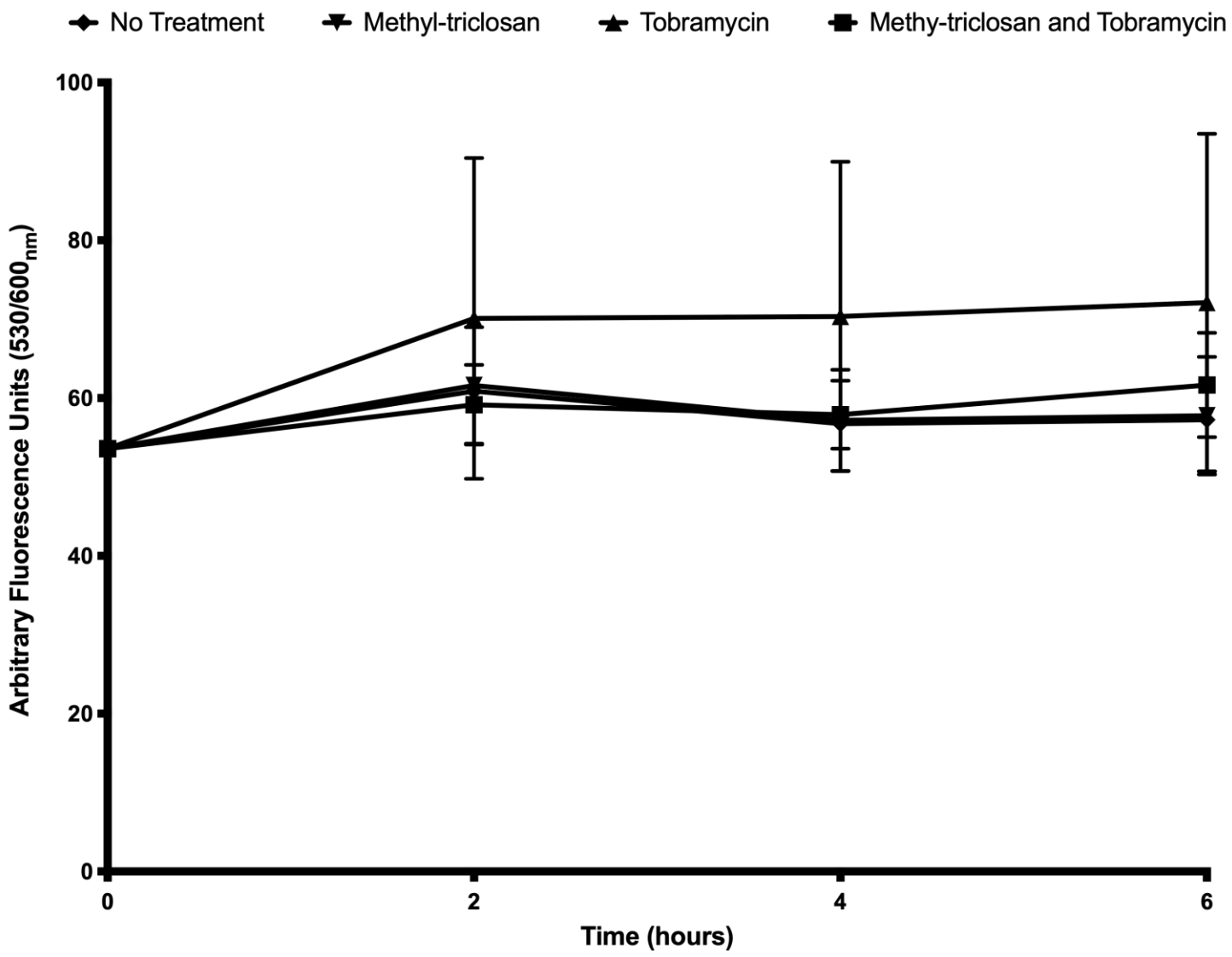


**FIG S5. Methyl-triclosan does not reduced RND-type efflux pump activity.** Ethidium bromide is a substrate of RND-type efflux pumps. 24-hr biofilms were stained with ethidium bromide to measure accumulation. Biofilms were treated with methyl-triclosan (100 µM) and tobramycin (500 µM) alone and in combination. Fluorescence was read at 0,2,4, and 6-hrs. The assay was performed three times in triplicate. Results represent the average arbitrary fluorescence units ±SEM.

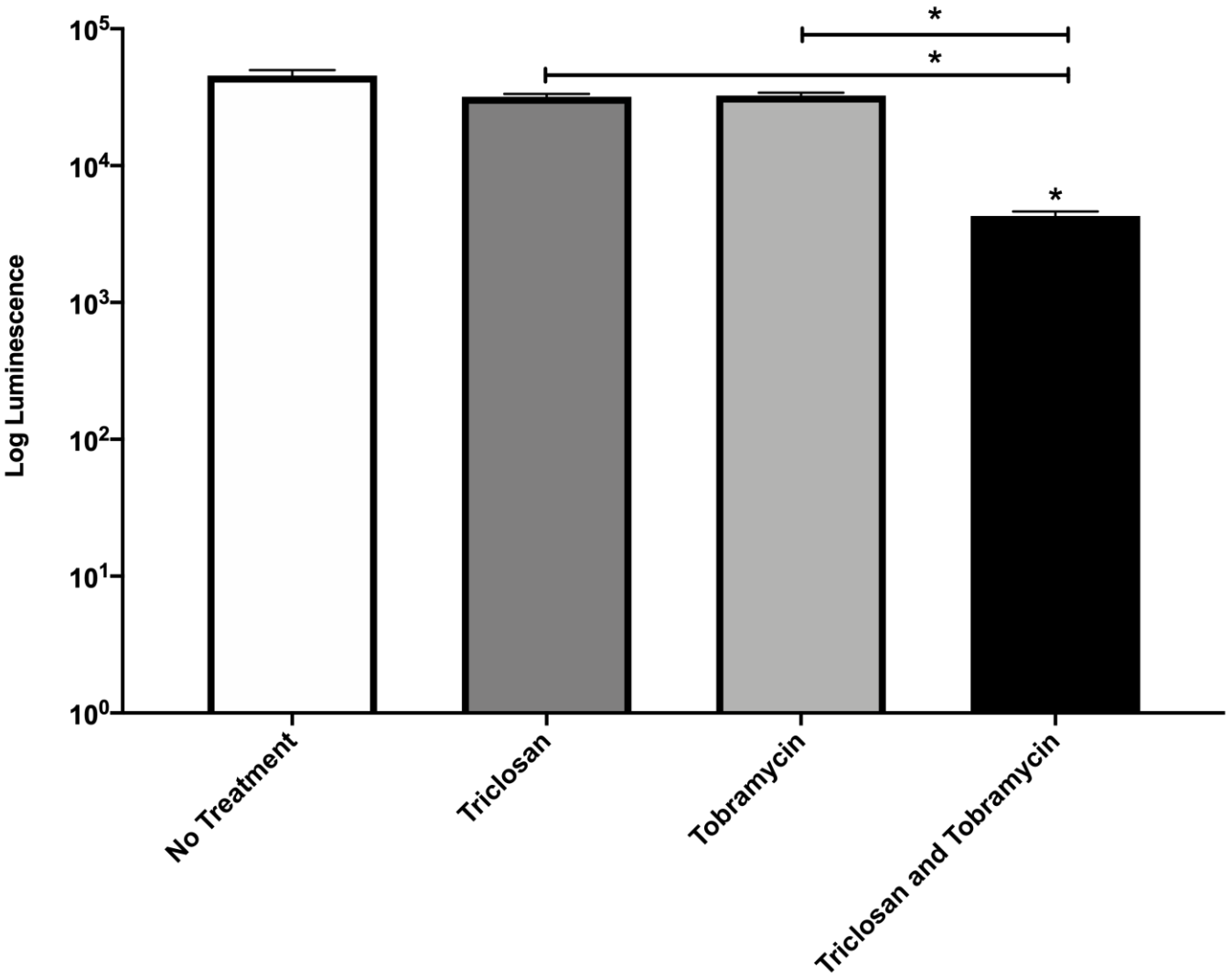


**FIG S6. DPBS starved biofilms are not more sensitive to tobramycin alone.** 24-hour old biofilms were starved of nutrients by replacing media with DPBS for 5-days. Starved biofilms were treated with triclosan (100 µM), or tobramycin (500 µM), alone and in combination for 6-hrs. The number of viable cells within the biofilms was quantified using the BacTiter-Glo™ assay. The assay was performed once using three biological replicates. The results represent the means plus the SEM. A one-way ANOVA followed by Sidak's multiple comparison post hoc test was used to determine statistical significance between the combination treatment and the untreated control and between triclosan alone or tobramycin alone and the combination treatment as indicated by the bars. *, $P < 0.05$.

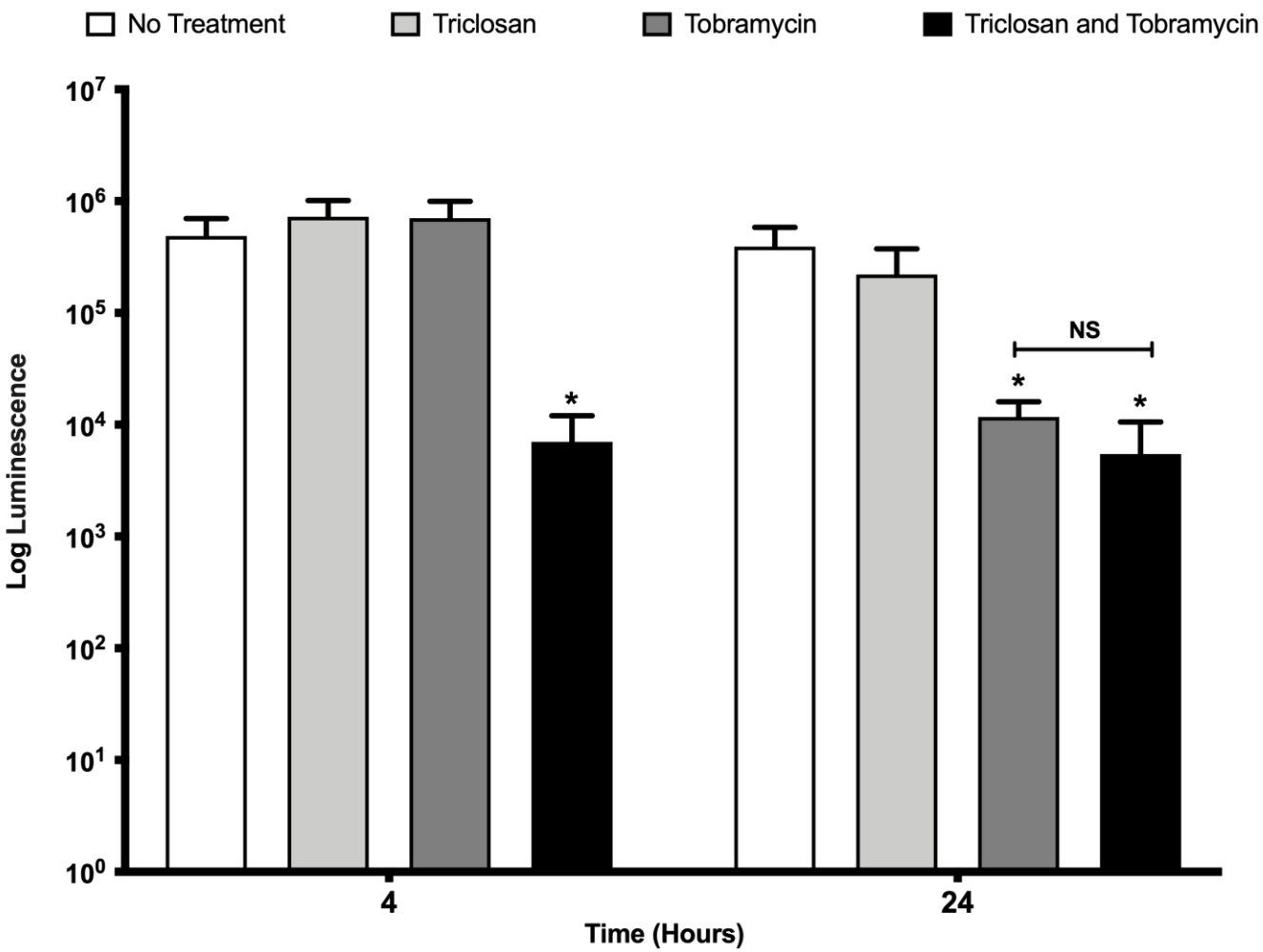


**FIG S7. Tobramycin is as effective as the combination after 24-hrs of treatment.** 24-hr old biofilms were treated for 24-hrs with triclosan (100 µM), tobramycin (500 µM), alone and in combination, and the number of viable cells within the biofilms were quantified by BacTiter-Glo™. The assay was performed at least three times in triplicate. The results represent means plus the SEM. A one-way ANOVA followed by Bonferroni's multiple comparison post-hoc test was used to determine statistical significance between untreated biofilms, tobramycin alone, and the combination treatment. In addition, using the same analysis, a comparison was made between tobramycin alone and the combination treatment. *, $P < 0.05$. NS, not significant. 4-hr treatments were previously published and are shown for comparison (28).

**Table S1.** Treatment regimens used for the selection of resistant mutants.

| Cycle | Tobramycin | Triclosan | Table Part A |
|---|---|---|---|
| 0 | 0 | 0 | |
| 1 | 0.00474756 | 0.47475615 | **Gradual Start** |
| 2 | 0.00678223 | 0.67822307 | |
| 3 | 0.0096889 | 0.9688901 | |
| 4 | 0.01384129 | 1.38412872 | |
| 5 | 0.01977327 | 1.97732674 | |
| 6 | 0.02824752 | 2.82475249 | |
| 7 | 0.04035361 | 4.0353607 | |
| 8 | 0.05764801 | 5.764801 | |
| 9 | 0.0823543 | 8.23543 | **Moderate Start** |
| 10 | 0.117649 | 11.7649 | |
| 11 | 0.16807 | 16.807 | |
| 12 | 0.2401 | 24.01 | |
| 13 | 0.343 | 34.3 | |
| 14 | 0.49 | 49 | |
| 15 | 0.7 | 70 | |
| 16 | 1* Tobramycin MIC | 100 | |

| Cycle | Tobramycin | Triclosan | Table Part B |
|---|---|---|---|
| 17 | 10 | 100 | **Gradual & Moderate** |
| 18 | 12.77 | 110.59 | |
| 19 | 16.30729 | 122.301481 | |
| 20 | 20.8244093 | 135.253208 | |
| 21 | 26.5927707 | 149.576523 | |
| 22 | 33.9589682 | 165.416676 | |
| 23 | 43.3656024 | 182.934302 | |
| 24 | 55.3778743 | 202.307045 | |
| 25 | 70.7175454 | 223.731361 | |
| 26 | 90.3063055 | 247.424512 | |
| 27 | 115.321152 | 273.626768 | |
| 28 | 147.265111 | 302.603843 | |
| 29 | 188.057547 | 334.64959 | |
| 30 | 240.149488 | 370.088981 | **End** |

27 *P. aeruginosa* biofilms serially passaged in parallel were exposed to sudden, moderate, and gradual treatment regimens consisting of ever-increasing concentrations of tobramycin and triclosan spread out over longer and longer periods of time, as shown in the table above. Gradual and moderate treatment groups were started at different concentrations of tobramycin and triclosan. However, they were then treated in subsequent cycles with ever increasing concentrations of triclosan and tobramycin at the same rate. For example, the moderate treatment group reached 1 µM of tobramycin and 100 µM of triclosan in 8-cycles, whereas the gradual treatment group reached the same concentration in 16-cycles from their initial treatments. The sudden treatment series was treated with 500 µM of triclosan and tobramycin from cycle day 1 and was eradicated, thus, is not shown in the table. MIC, minimum inhibitory concentration.